PBPK Modeling for Hepatically Impaired Patients

Annika Schneider, Bayer AG

OSP community conference 2024

Liver cirrhosis

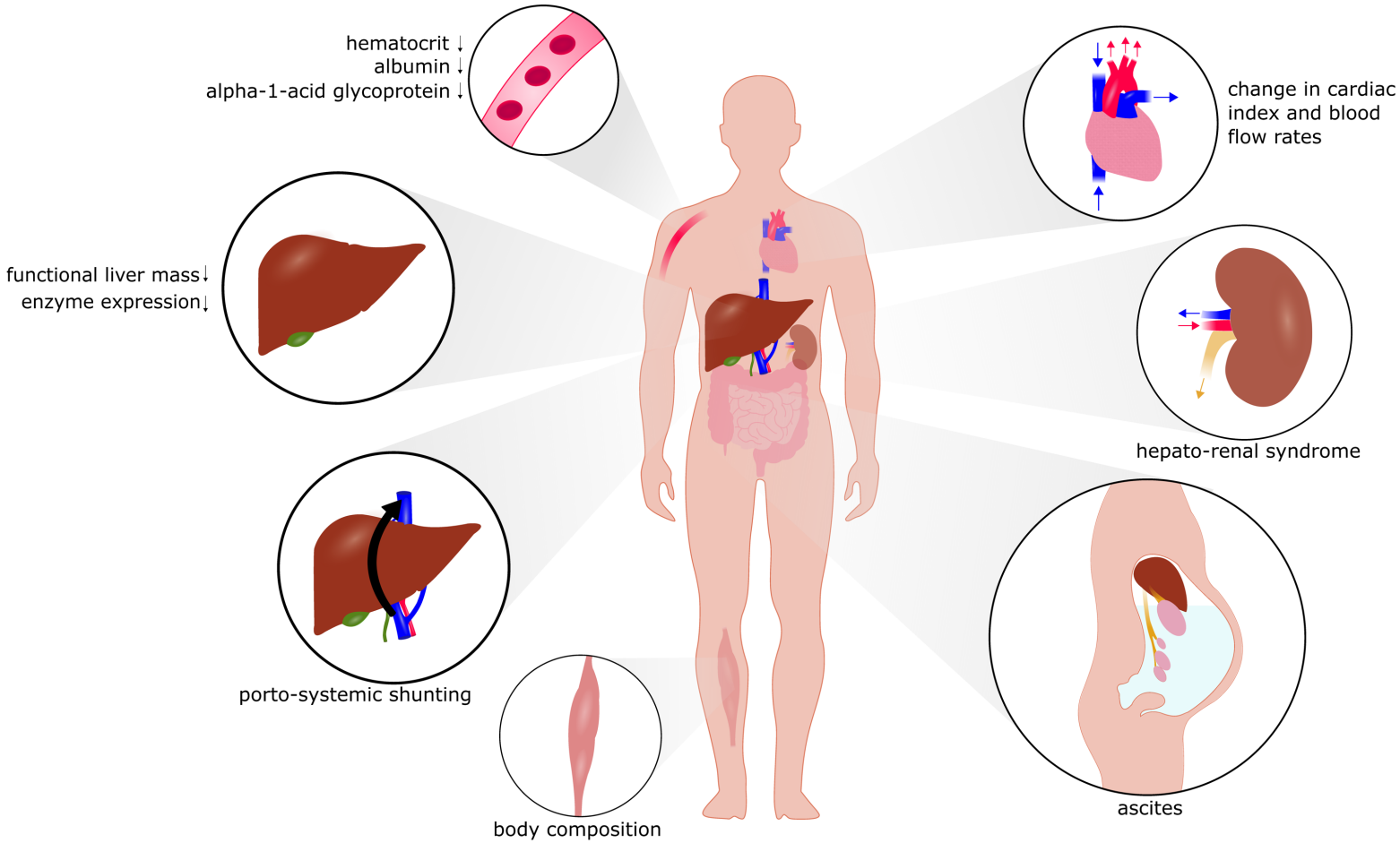

Figure source: Schneider 2024

Liver cirrhosis - Child-Pugh score

Points	1	2	3
Encephalopathy	None	Moderate	Severe
Ascites	Absent	Slight	Moderate
Bilirubin [mg/dL]	<2	2.1-3	>3
Albumin [g/dL]	>3.5	2.8-3.5	<2.8
Prothrombin time (seconds > control)	0-3.9	4-6	>6

Child-Pugh Score	Child- Pugh Grade	Life expectancy (years)
5-6	A	15-20
7-9	B	4-14
10-15	C	1-3

Motivation

- Regulatory agencies recommend performing PK studies in patients with hepatic impairment for
  - Drugs that have a high probability of being administered to these patients
  - Drugs that have at least a fraction metabolized of 20%
  - Drugs that are excreted via bile
  - Drugs with a narrow therapeutic window
- Clinical studies in hepatically impaired patients are expensive and patient recruitment can be challenging
- Modeling to supplement clinical studies, guide study design, and patient stratification, or even replace clinical studies

PBPK modeling for hepatically impaired patients

Current status

Edginton & Willman 2008

Table I. Physiological changes associated with liver cirrhosis

Parameter	Child-Pugh class		
	A	B	C
Blood flow			
portal[a]	0.40	0.36	0.04
hepatic arterial[b]	1.3	2.3	3.4
renal[c]	0.88	0.65	0.48
other organs[d]	1.75	2.25	2.75
Cardiac index[e]	1.11	1.27	1.36
Albumin[f]	0.81	0.68	0.50
α_1-Acid glycoprotein[g]	0.60	0.56	0.30
Haematocrit value[h]	0.39	0.37	0.35
Functional liver mass[i]	0.69	0.55	0.28
Hepatic enzymes[j]			
CYP3A4	1	0.4	0.4
CYP1A2	1	0.1	0.1
CYP2E1	1	0.83	0.83
GFR[k]	1	0.70	0.36

Johnson 2010

Table III. Physiological and biochemical parameter changes associated with liver cirrhosis

Parameter	Control	Child-Pugh score		
		A	B	C
Liver volume fraction	1.0	0.81	0.65	0.53
CYP (ρmol/mg)				
1A2	52	32.9	13.6	6.10
2A6	20	17.7	12.3	6.40
2B6	17	17.0	15.3	13.6
2C8	24	16.6	12.5	7.90
2C9	73	50.4	38.0	24.1
2C18	1.0	0.32	0.26	0.12
2C19	14	4.50	3.60	1.70
2D6	8.0	6.10	2.60	0.84
2E1	61	45.1	29.3	6.71
3A4	137	80.8	53.2	34.2
Gut CYP3A4 (nmol per total gut)	70	59	40	25
Albumin (g/L)	44.7	41.1	33.9	26.3
α_1-acid glycoprotein (g/L)	0.80	0.57	0.52	0.46
Haematocrit (%)	40.9	36.6	32.9	31.9
Cardiac output (L/h)	306	355	403	431
Portal blood flow (L/h)				
males	58.2	52.9	36.9	32.2
females	65.8	59.9	41.7	36.4
Hepatic arterial blood flow (L/h)	19.9	28	32.3	38.1
Q_{villi} (L/h)	18.4	23.7	28.0	36.6
GFR (mL/min)	120	83.7	69.9	66.5

CYP = cytochrome P450; **GFR** = glomerular filtration rate; Q_{villi} = villous blood flow.

Heimbach 2021 (SimCyp V15)

Table S5. Physiological Differences between Healthy Volunteers and Patients with Liver Cirrhosis[a]

Liver condition	Healthy Control	Mild Impairment	Moderate Impairment	Severe Impairment
Simcyp-population	HV	CP-A	CP-B	CP-C
CYP3A4 abundance in the liver (pmol /mg)	137	108	56	31
CYP3A4 abundance in the intestine (pmol /mg)	66.2	55.8	37.8	23.6
CYP2D6 abundance (EM) in the liver (pmol /mg)	8.0	6.1	2.6	
CYP2D6 abundance (EM) in the intestine (pmol /mg)	2.5	1.91	0.81	
Liver Volume (L)	1.65	1.47	1.17	1.0
Liver Q (Arterial/Portal), (% cardiac output)	6.5/19	9.2/17.3	10.6/13.6	12.5/10.5
Kidney Q (% cardiac output)	19	16.7	12.4	9.2
Gastric residence time (hr) (fasted /fed)/colon transit time	0.4/1.0/12	0.48/1.2/24	0.55/1.38/24	0.6/1.5/24
Albumin/a1-AG/Haematocrit (ratio to HV, male)	1 / 1/1	0.8 /0.9/0.9	0.7 /0.8/0.8	0.6/0.6/0.8

[a] Simcyp V15. Other differences include the abundance of other Cyps in the liver and the intestine, tissue volumes folds scalar, serum creatinine, blood flow rate in brain and muscle. Differences in gastrointestinal absorption, bile acid output rate or bile acid composition are not included in the PBPK model. There are no difference in abundance of transporters, CES1, CES2 and UGTs. Table modified from Certara.

PBPK modeling for hepatically impaired patients

Current status

- 2019-2023: 74 of 243 approved novel drug applications to the FDA included PBPK modelling
  - 5 utilized PBPK models to predict the impact of hepatic impairment on PK
- Child-Pugh score was not designed to estimate the impact of the disease on drug PK, but used as a classification system in 95% of PK studies in hepatic impairment populations in drug development
- Literature identified gaps in the pathophysiology models e.g., missing implementation of ascites, changes in body composition and unknown sources of PK variability

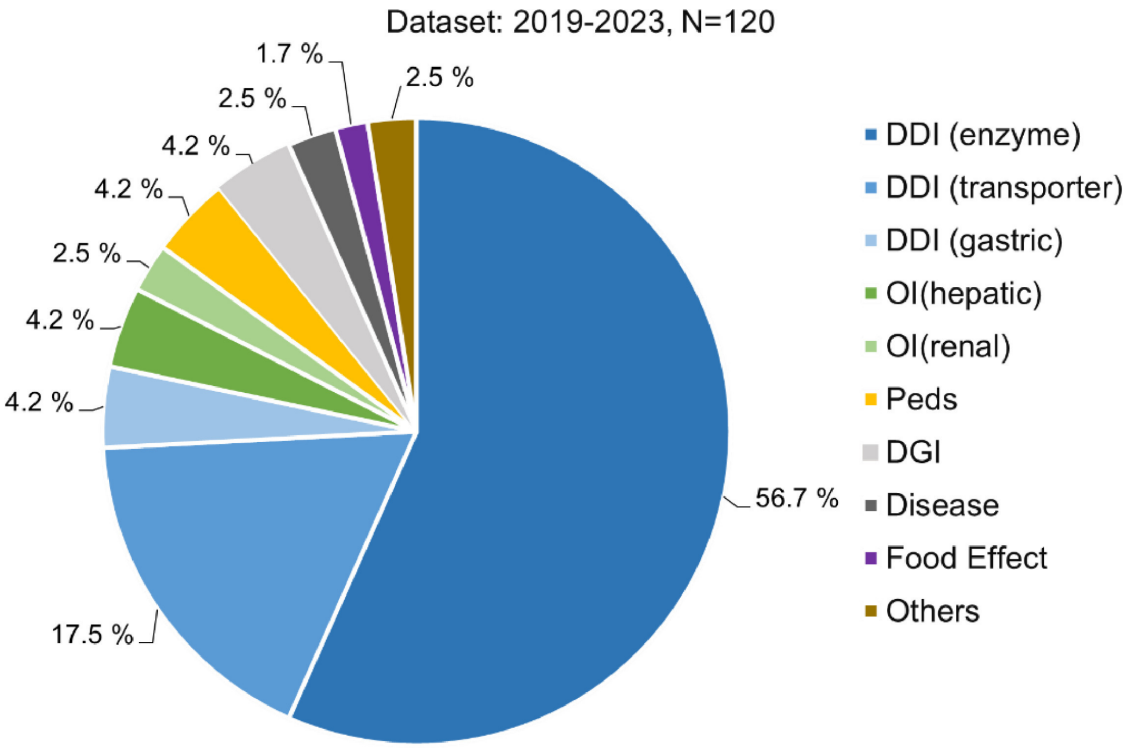

Figure source: Sun et al. 2024

Pathophysiological changes in liver cirrhosis

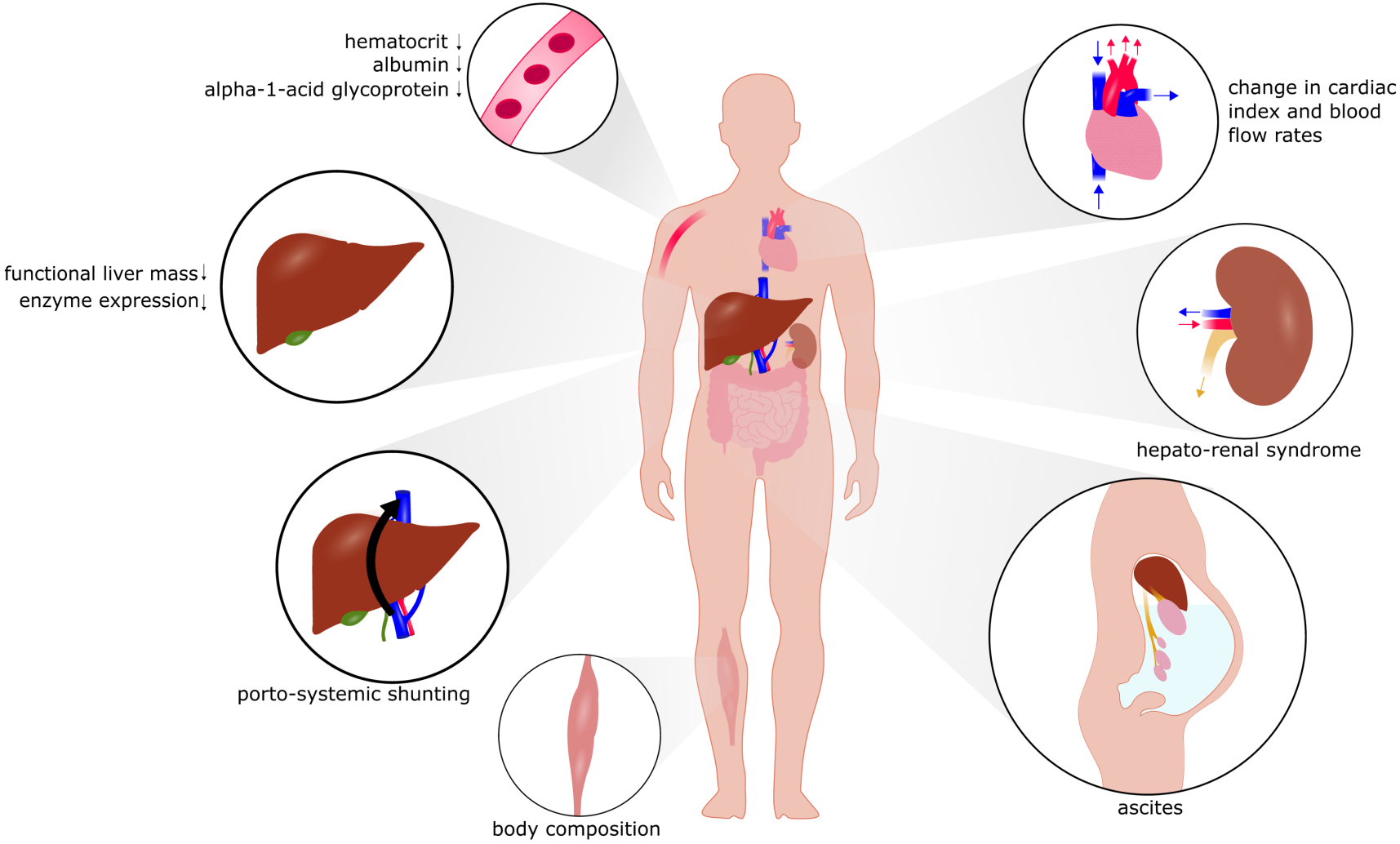

Figure source: Schneider 2024

Workflow quantifying continous disease progression

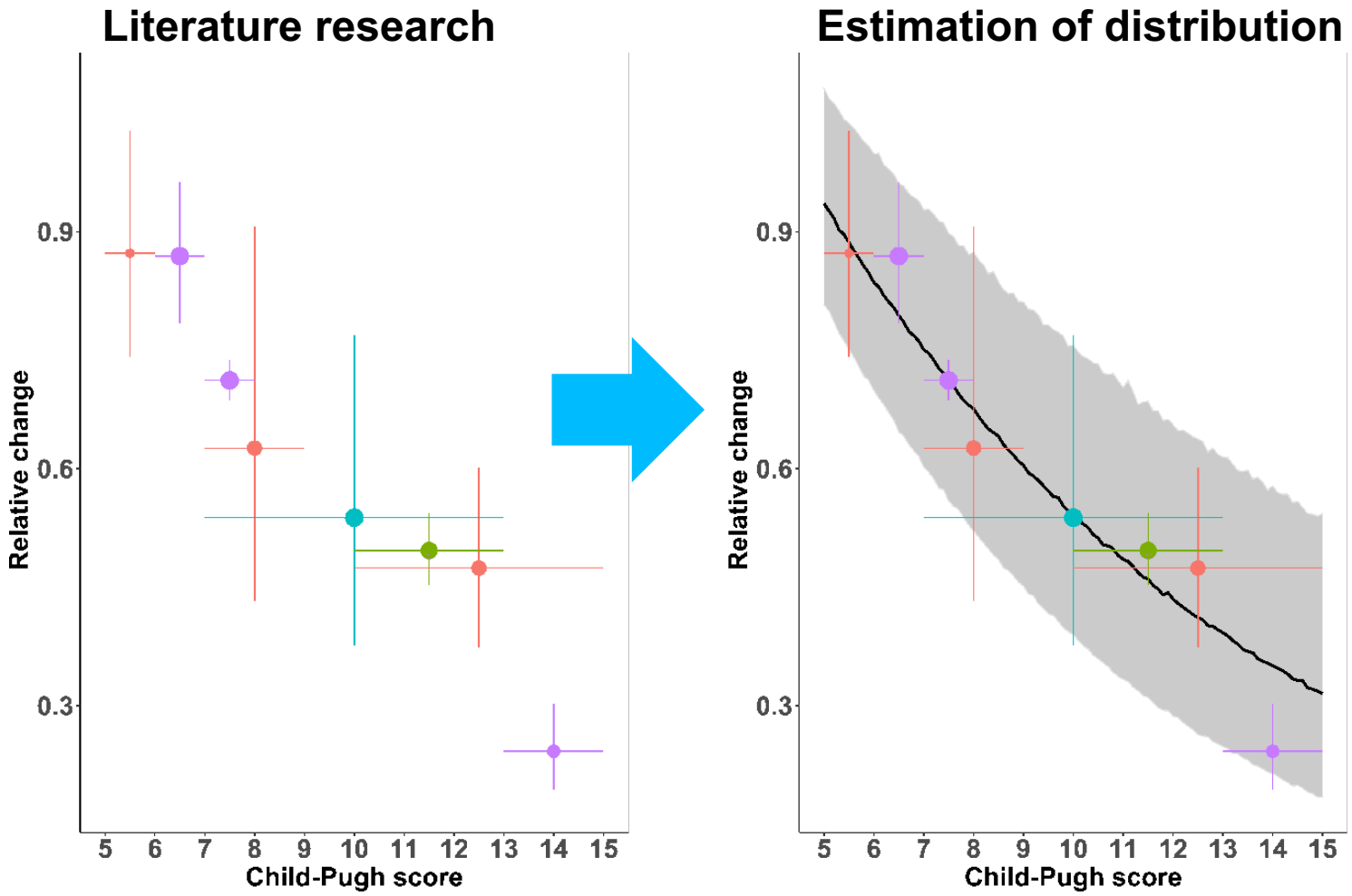

Markov chain Monte Carlo (MCMC)-based approach

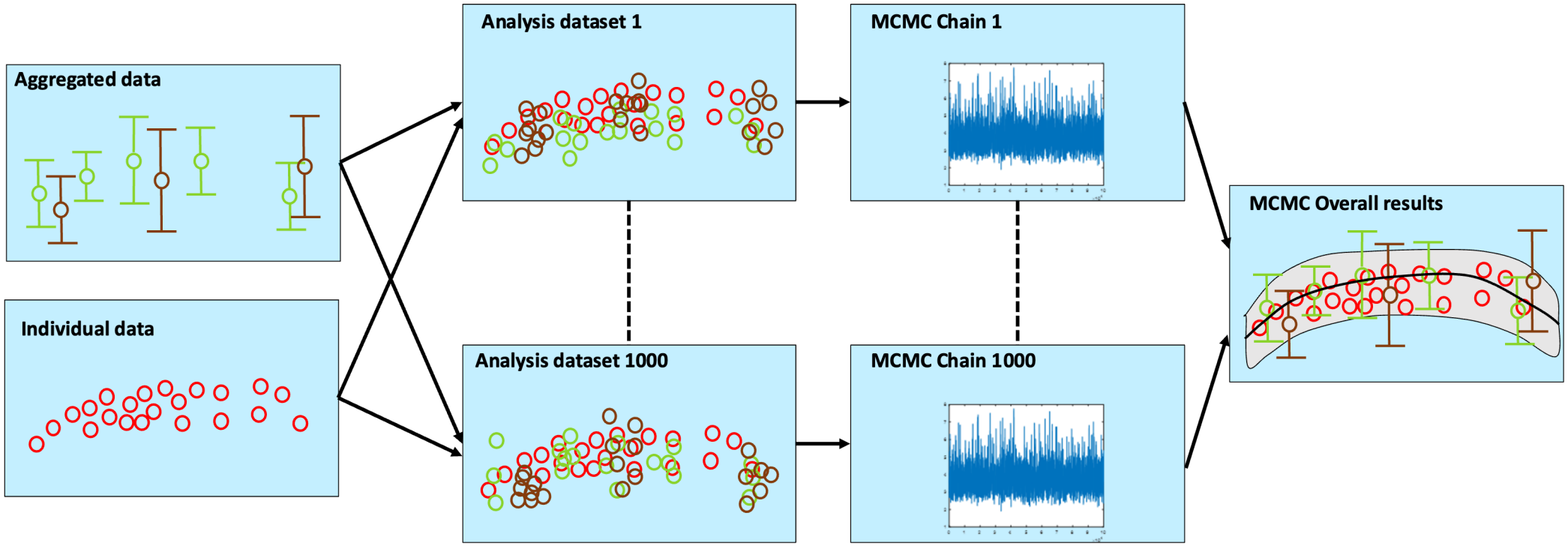

Figure source: Mayer et al. 2018

Repository for hepatic impairment pathophysiology

- **30** physiological **parameters** (including “new” parameters such as body composition)
- Quantified **mean** changes as well as population **variability**, continuous throughout the disease progression
- Based on **216,609 data points** from 68 literature studies and 71,646 patients from electronic health record data

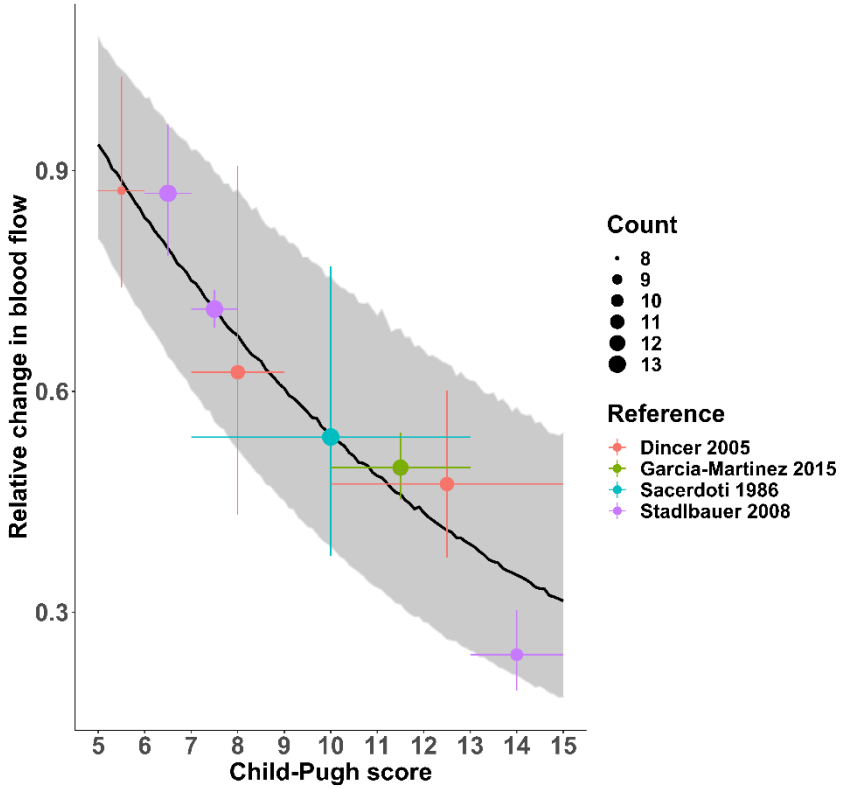

Figure source: Schneider 2024

Virtual population generation

- Creation of virtual populations according to reported demographics, Child-Pugh score and disease information e.g. ascites/ non-ascites etc.
- Assumption: Correlation between the severeness of pathophysiological changes
- Structural changes to implement ascites and shunting

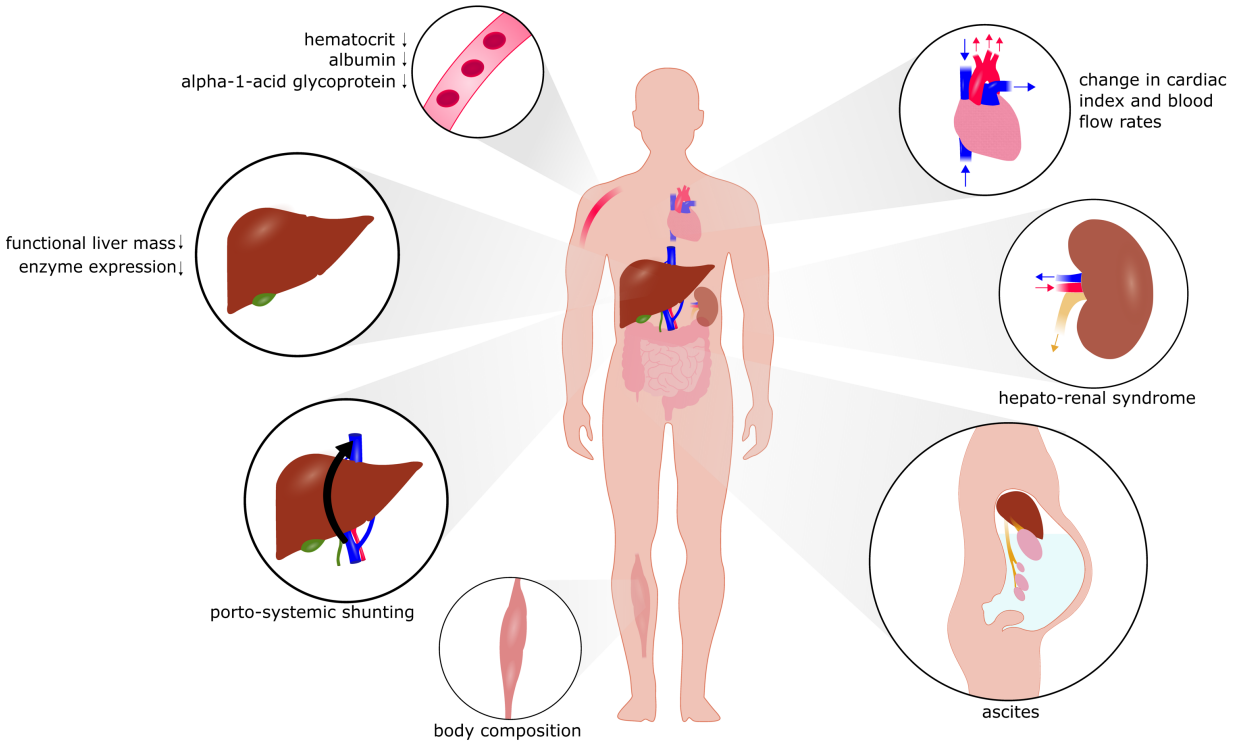

Figure source: Schneider 2024

Simulation results

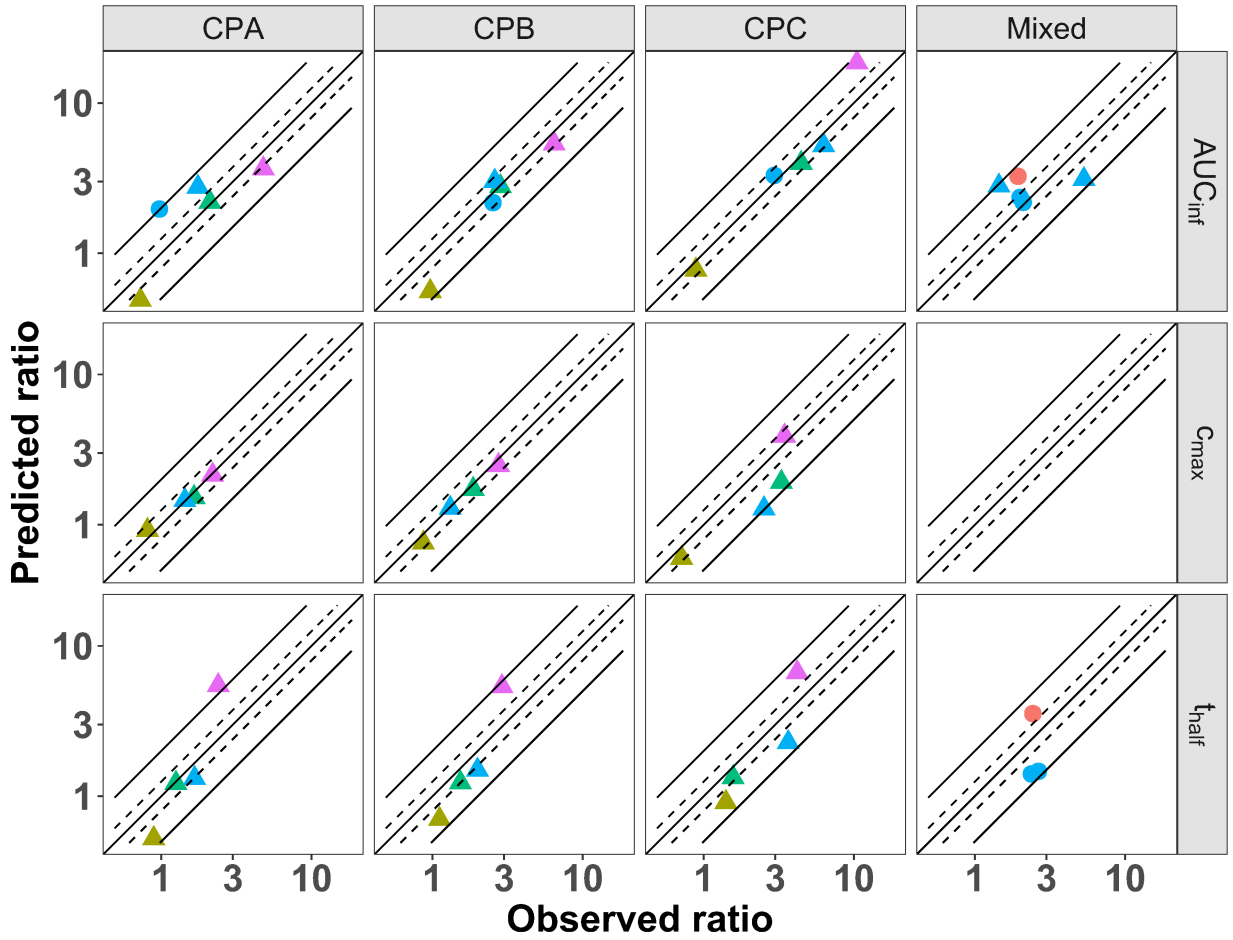

Compound

- alfentanil
- efavirenz
- metoprolol
- midazolam
- omeprazole

Route

- IV
- PO

solid lines: line of identity and the twofold prediction interval
dashed lines: 0.8- and 1.25-fold prediction interval
CPA – Child-Pugh A, CPB – Child-Pugh B, CPC – Child-Pugh C

Figure source: Schneider 2024

Conclusion

- Repository quantifying 30 physiological parameters
- Quantified mean changes as well as population variability, continuous throughout the disease progression
- Based on 216,609 data points from 68 literature studies and 71,646 patients from electronic health record data
- Good simulation performance with several probe drugs
- Open topics: intestinal enzyme expression, transporter expressions, correlations between pathophysiology, further unknown mechanisms

References

Edginton AN, Willmann S. Physiology-based simulations of a pathological condition: prediction of pharmacokinetics in patients with liver cirrhosis. Clin Pharmacokinet. 2008;47(11):743-52. doi: 10.2165/00003088-200847110-00005. PMID: 18840029.

Heimbach T, Chen Y, Chen J, Dixit V, Parrott N, Peters SA, Poggesi I, Sharma P, Snoeys J, Shebley M, Tai G, Tse S, Upreti VV, Wang YH, Tsai A, Xia B, Zheng M, Zhu AZX, Hall S. Physiologically-Based Pharmacokinetic Modeling in Renal and Hepatic Impairment Populations: A Pharmaceutical Industry Perspective. Clin Pharmacol Ther. 2021 Aug;110(2):297-310. doi: 10.1002/cpt.2125. Epub 2020 Dec 30. PMID: 33270249; PMCID: PMC8359227.

Johnson TN, Boussery K, Rowland-Yeo K, Tucker GT, Rostami-Hodjegan A. A semi-mechanistic model to predict the effects of liver cirrhosis on drug clearance. Clin Pharmacokinet. 2010 Mar;49(3):189-206. doi: 10.2165/11318160-000000000-00000. PMID: 20170207.

Mayer, H., Burghaus, R., Coböken, K., Frenchen, S., Ince, I., Schlender, J., 2018. A novel approach to estimate ontogenies for PBPK applications–from literature data to simulations. Population Approach Group Europe (PAGE), 27th PAGE Annual Meeting< https://www.page-meeting.org/default.asp

Schneider, Annika R. P.; Model-informed treatment optimization of liver cirrhosis patients, 2024; doi: 10.18154/RWTH-2024-01771

Sun Z, Zhao N, Zhao X, Wang Z, Liu Z, Cui Y. Application of physiologically based pharmacokinetic modeling of novel drugs approved by the U.S. food and drug administration. Eur J Pharm Sci. 2024 Sep 1;200:106838. doi: 10.1016/j.ejps.2024.106838. Epub 2024 Jul 1. PMID: 38960205.

Thank you!

Bye-Bye

Backup

Table of content

// Liver cirrhosis and the Child-Pugh score

// Motivation

// Current modelling approaches

// A new pathophysiological repository

// Simulation results

// Summary & conclusion

Fitted pathophysiological changes in comparison to published repositories

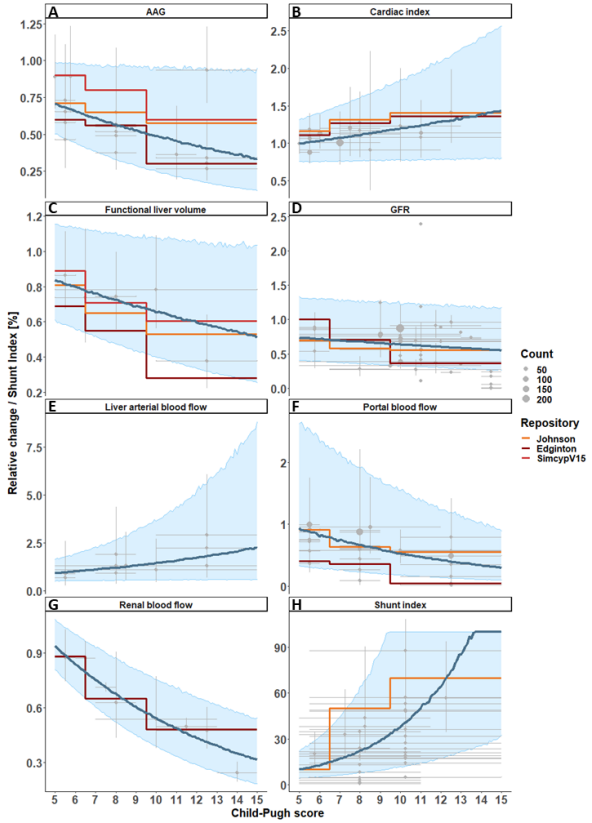

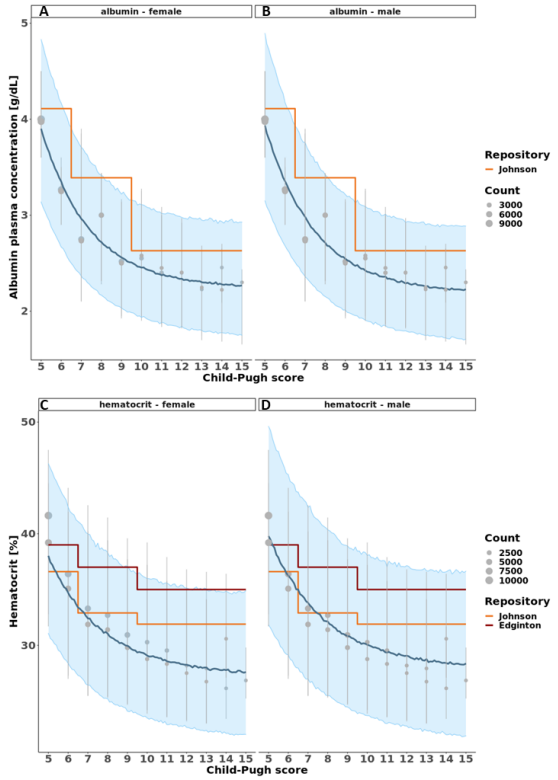

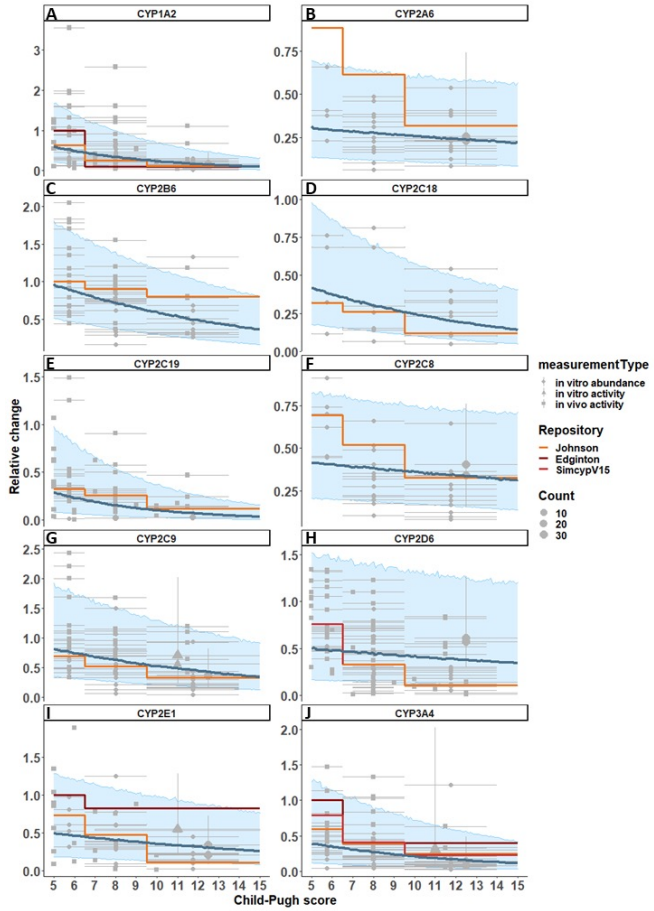

Figure source: Schneider 2024

Fitted pathophysiological changes in comparison to published repositories

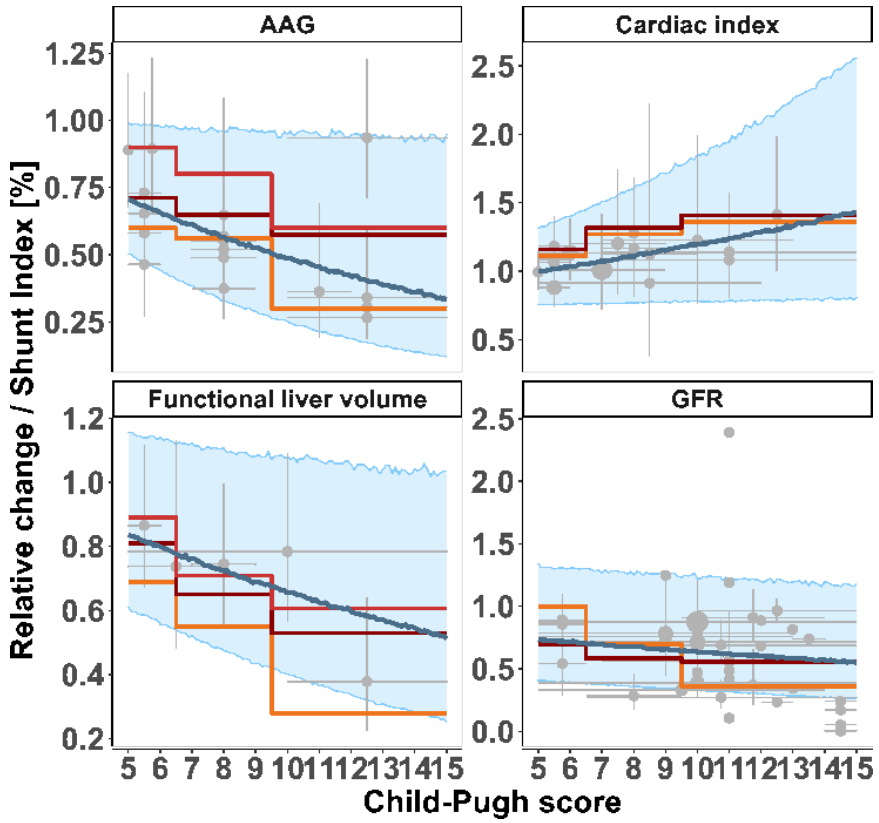

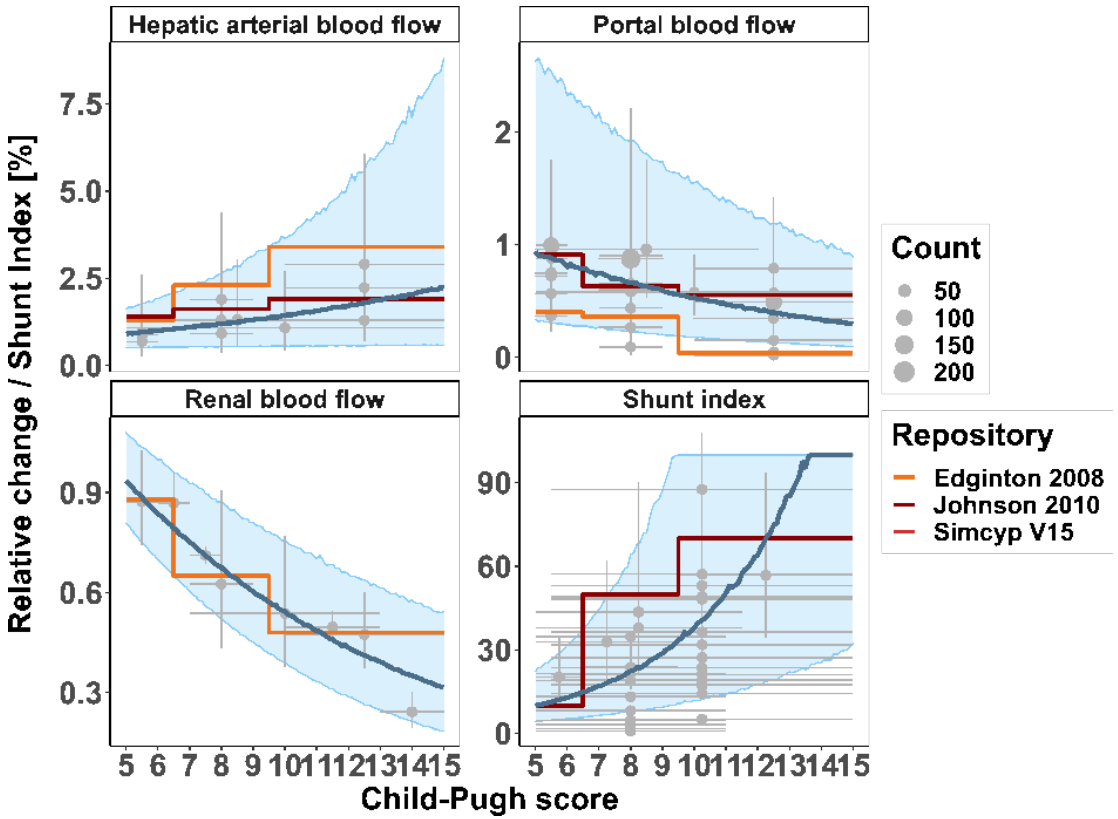

Figure source: Schneider 2024

Body compositon & ascites

Plasma volume

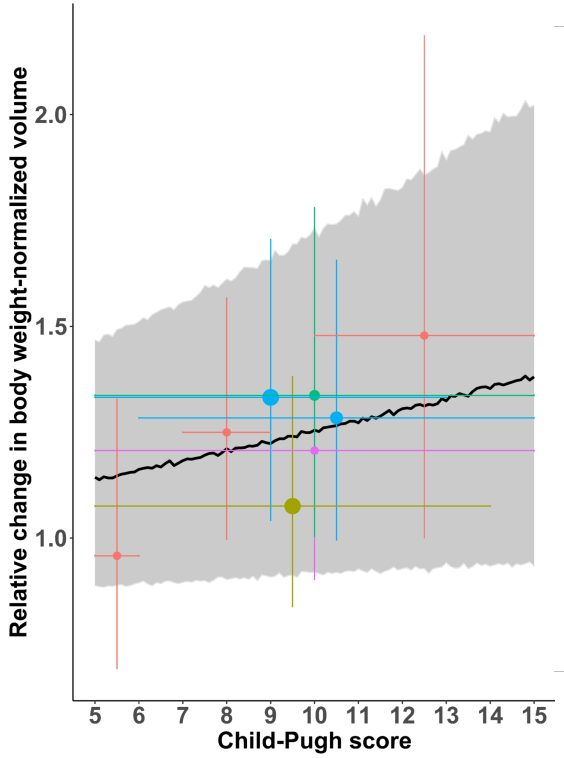

Muscle volume

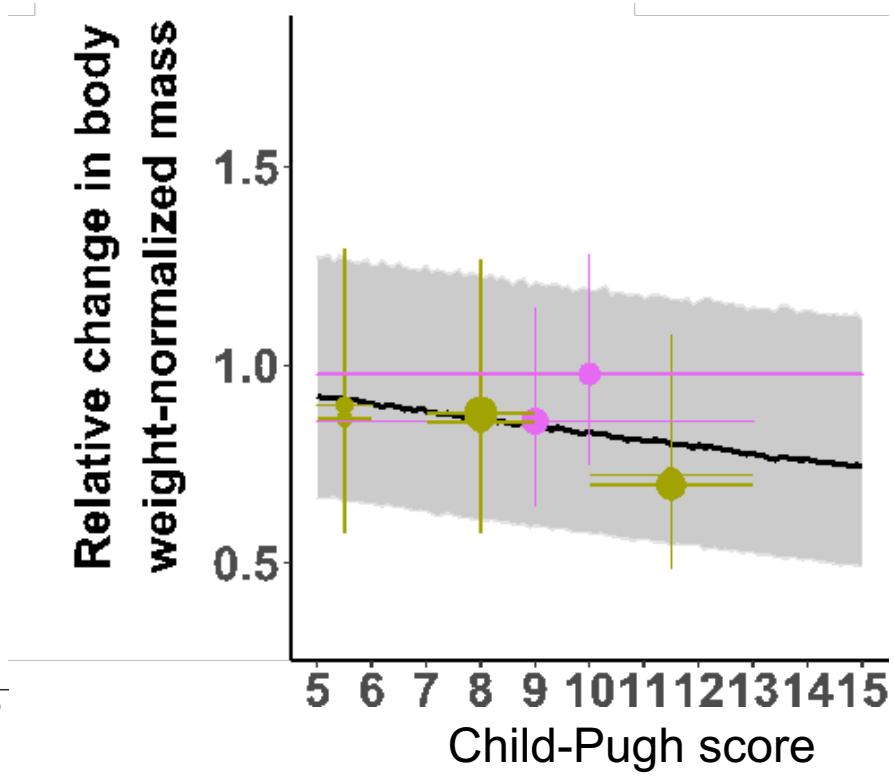

Fat volume

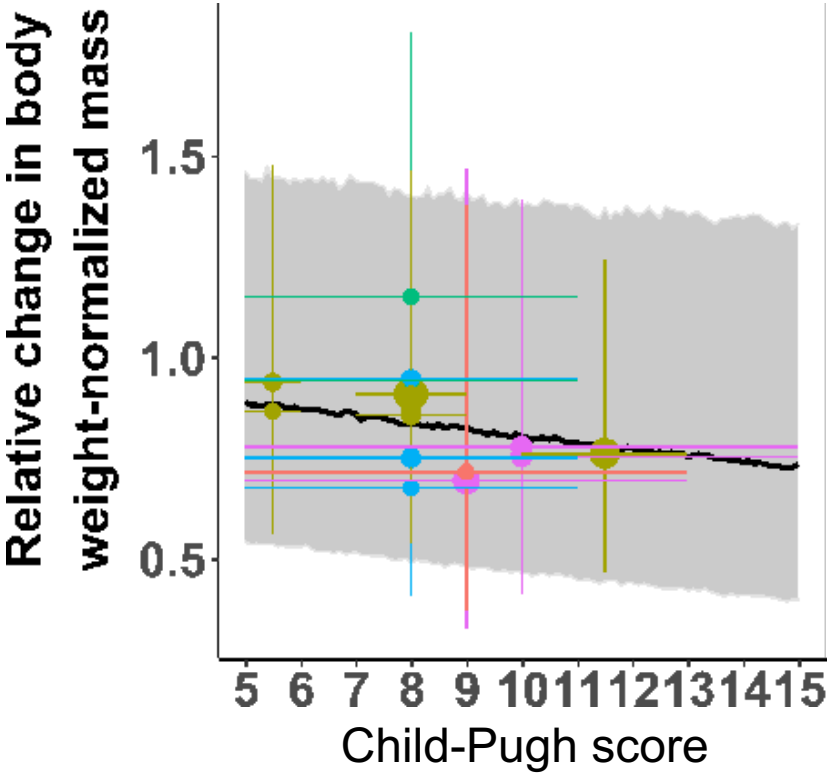

Figure source: Schneider 2024

Body compositon & ascites

Prevalence of ascites within a cirrhotic population

Child-Pugh score	Ascites frequency [% of cirrhotic population]
5	0.0
6	0.1
7	12.9
8	44.5
9	59.2
10	64.1
11	79.7
12	99.5
13	99.9
14-15	100.0

Extracellular body water (ECW)

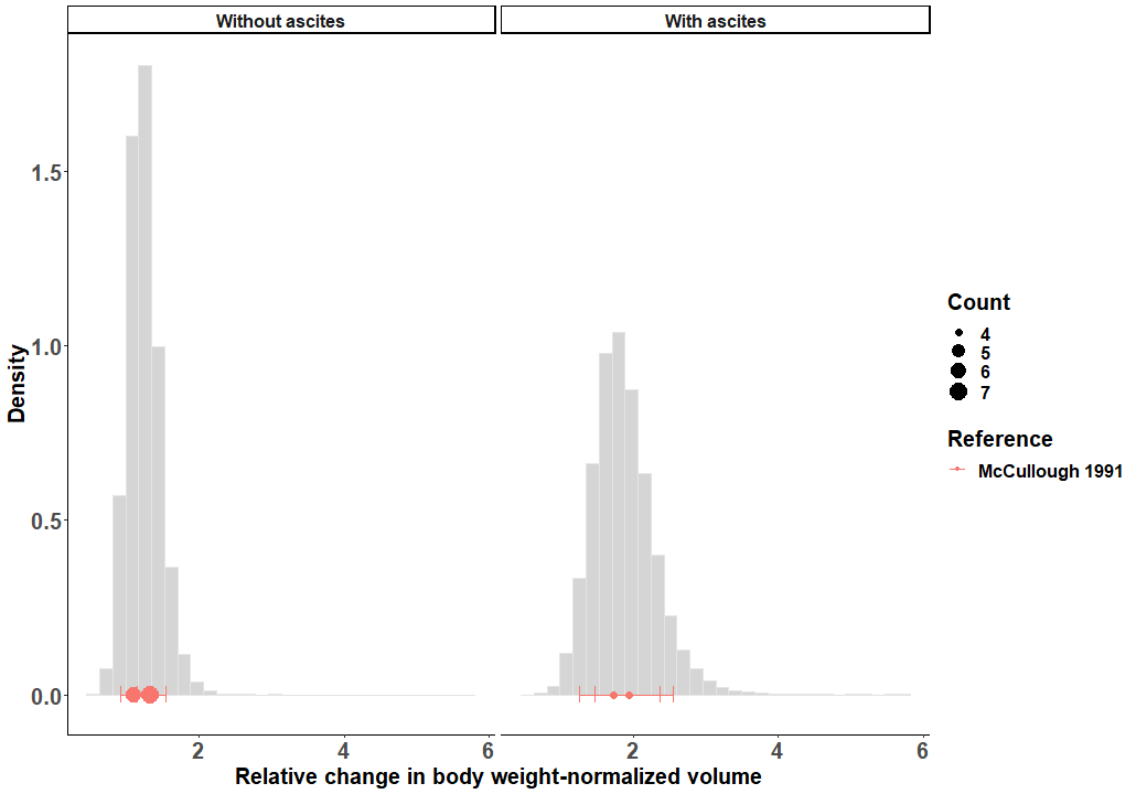

Table source: Schneider 2024

Shunting

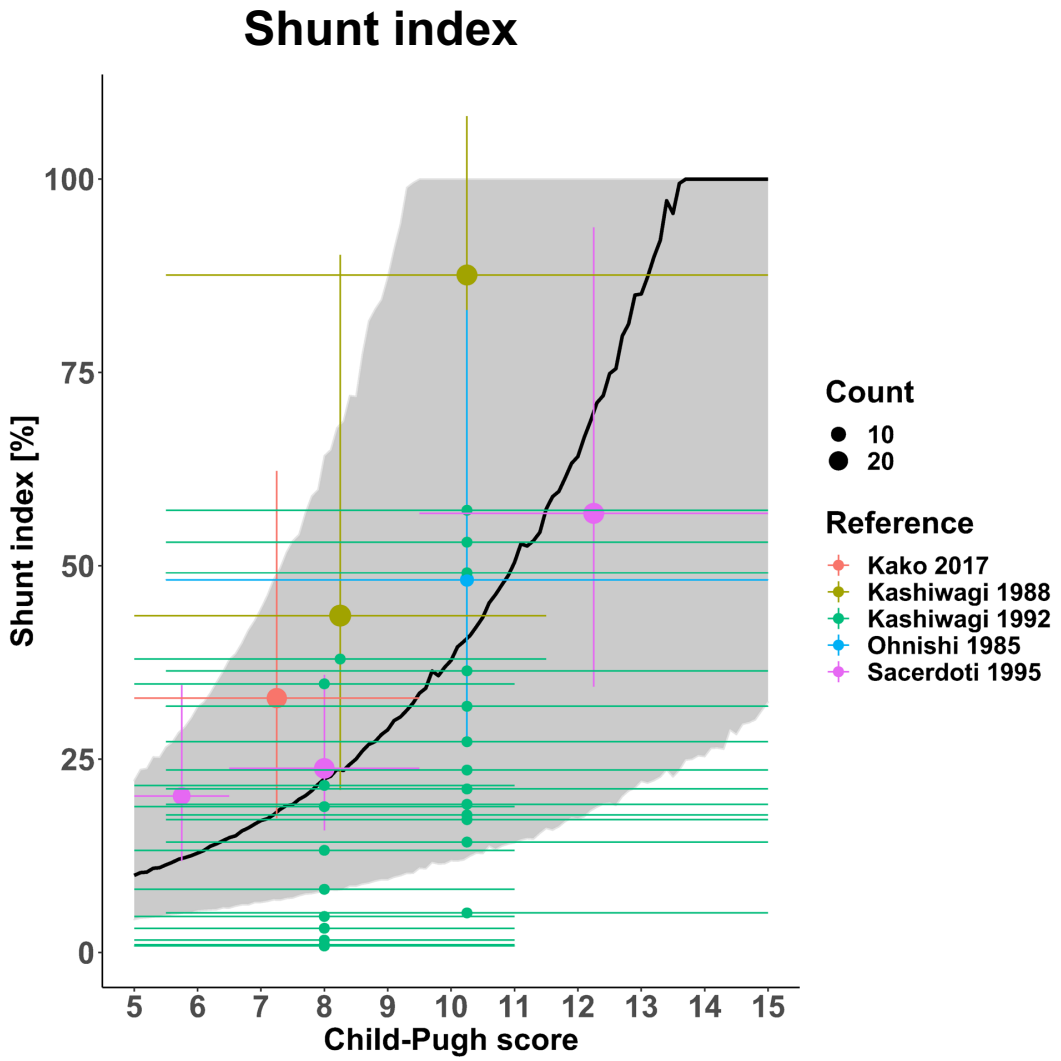

Shunt frequency

Child-Pugh A	Child-Pugh B	Child-Pugh C
42.4%	58.9%	71.1%

Figure & table source: Schneider 2024

Body compositon & ascites

Plasma volume

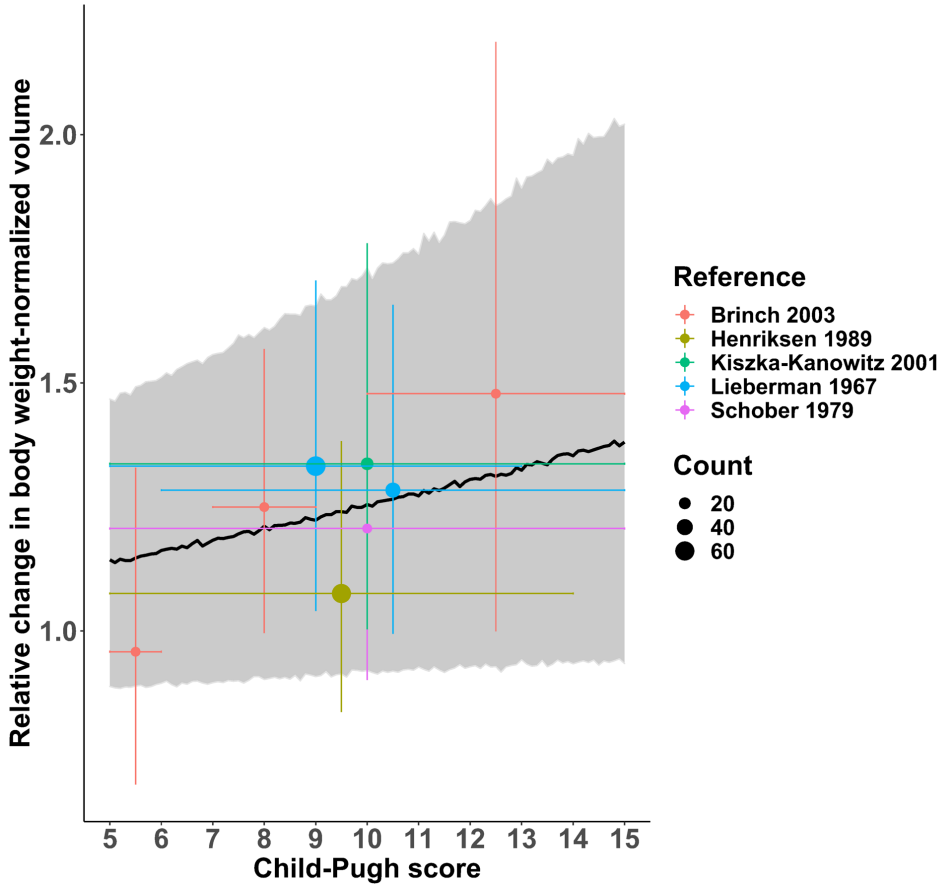

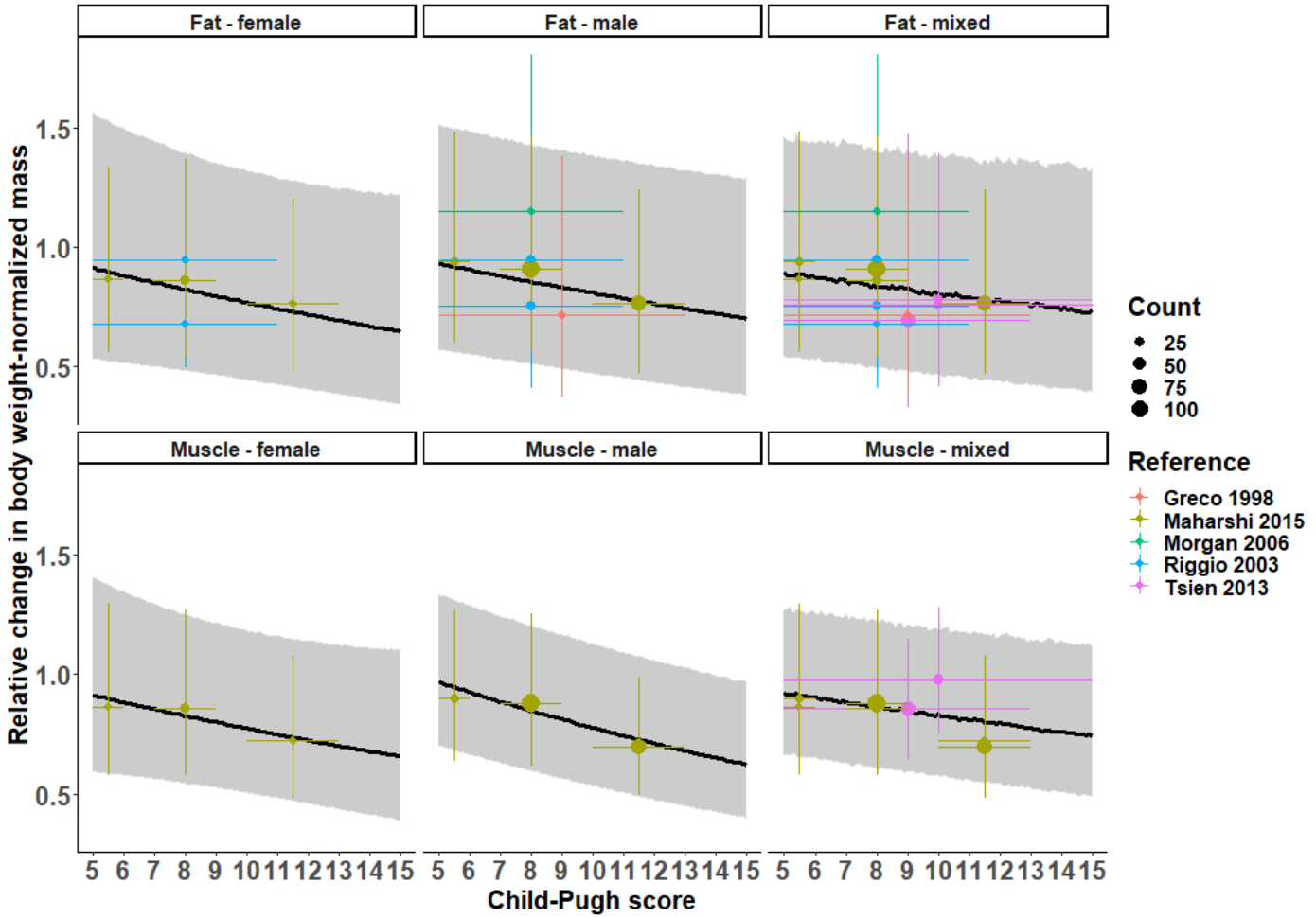

Figure source: Schneider 2024

Body compositon & ascites

Prevalence of ascites within a cirrhotic population

Child-Pugh score	Ascites frequency [% of cirrhotic population]
5	0.0
6	0.1
7	12.9
8	44.5
9	59.2
10	64.1
11	79.7
12	99.5
13	99.9
14-15	100.0

Ascites grading

Grade	Definition	Volume
Grade 1	Mild ascites; only detectable by ultrasound	> 100 mL
Grade 2	Moderate ascites evident by proportionate sensible abdominal distention	> 1,000 mL
Grade 3	Large ascites with marked abdominal distention	Liters

Table source: Schneider 2024

Enzymes

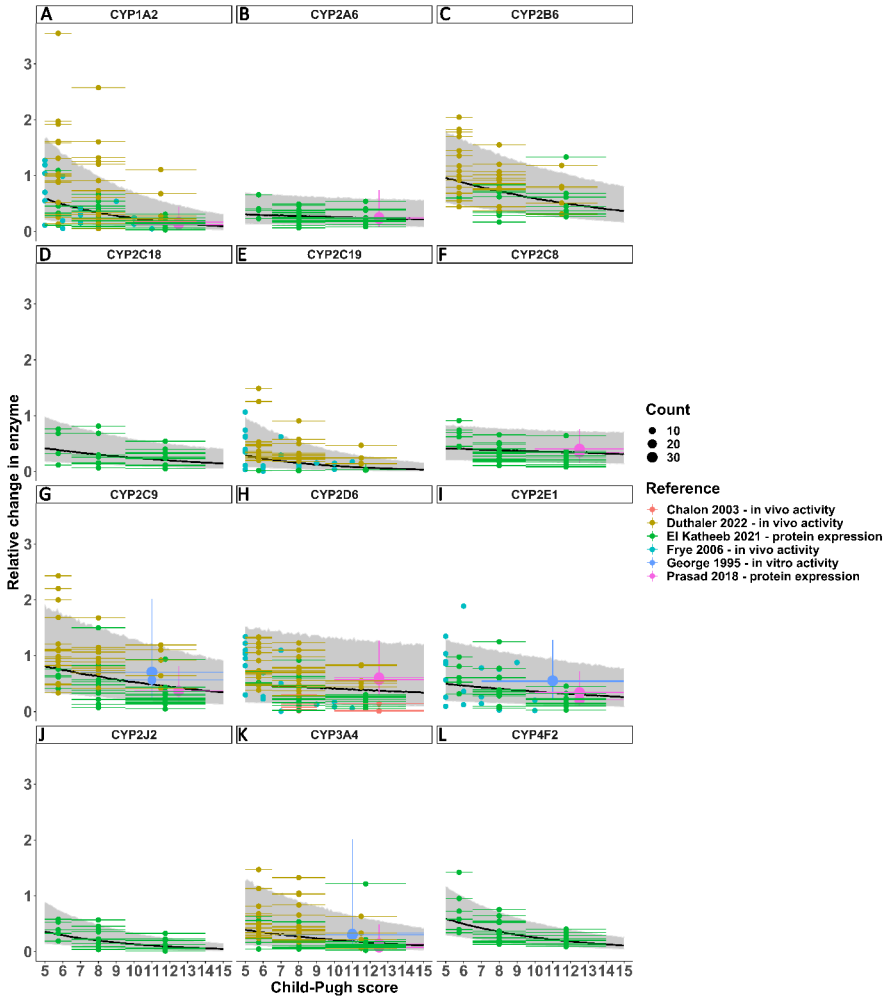

Figure source: Schneider 2024

Hematocrit

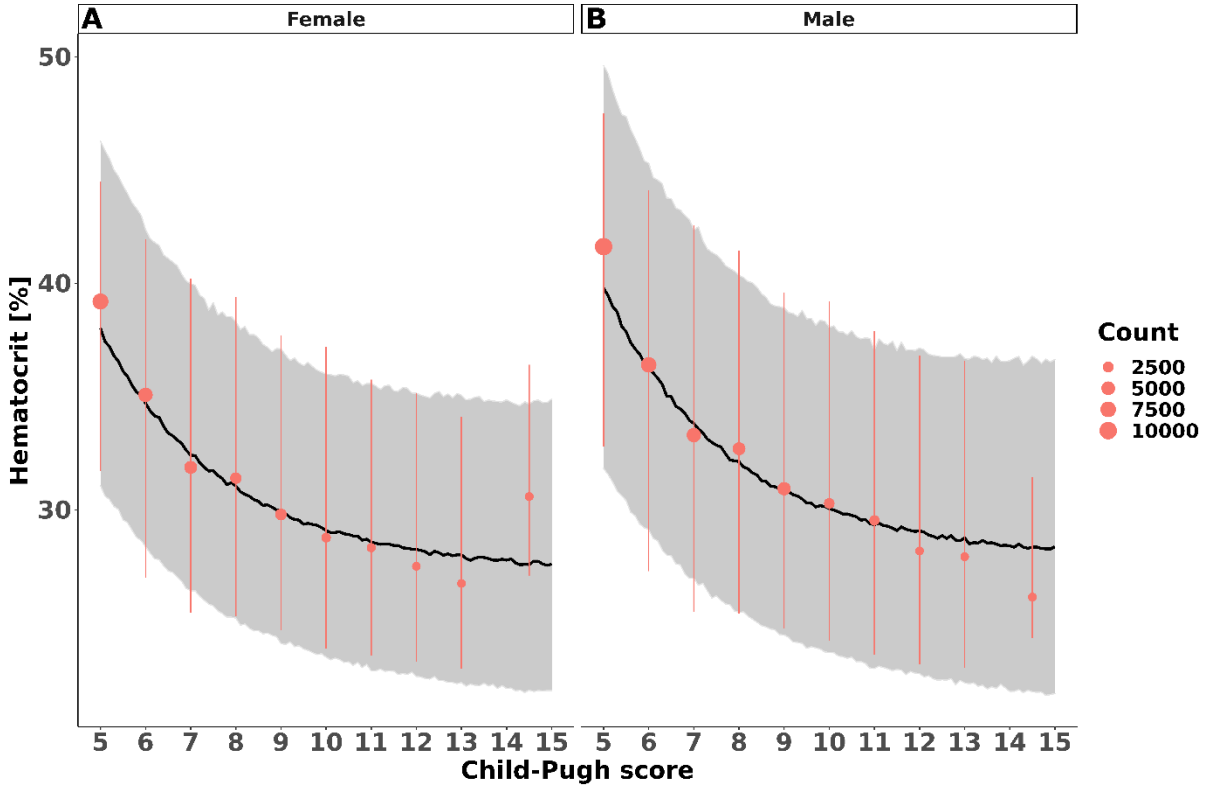

Figure source: Schneider 2024

Albumin

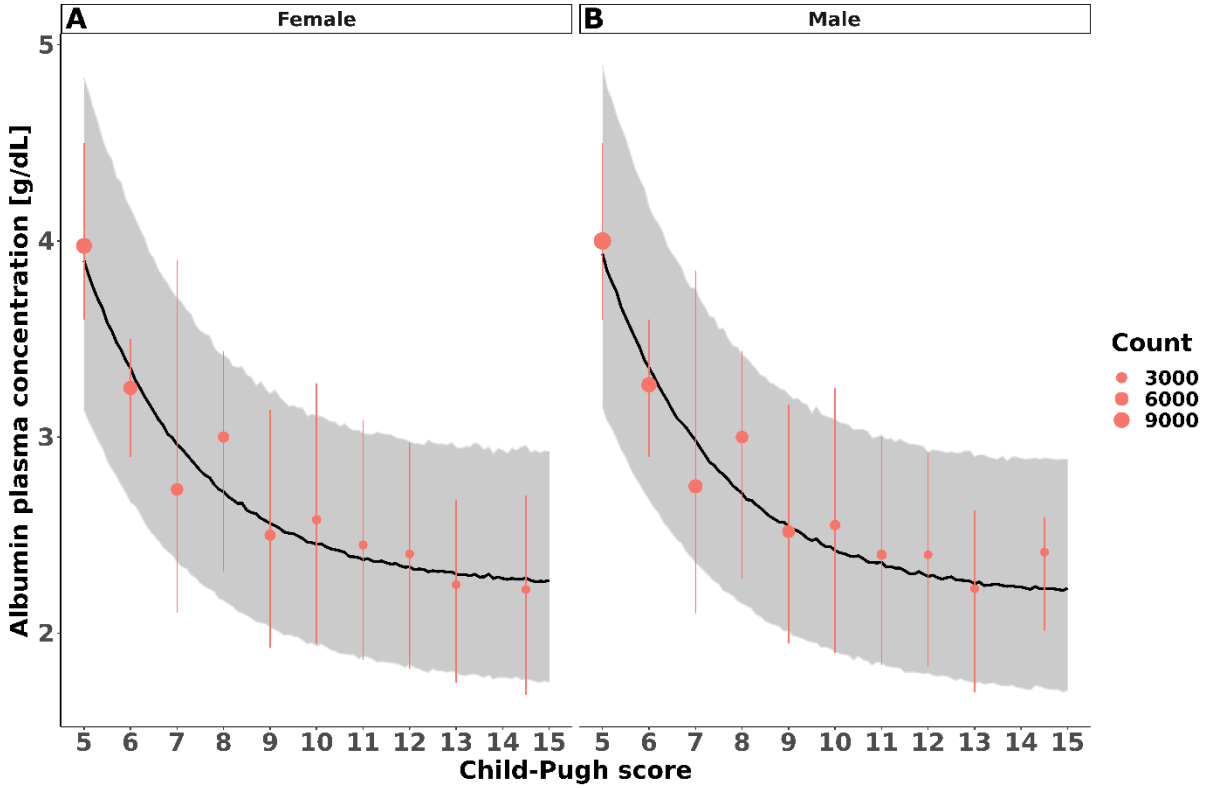

Figure source: Schneider 2024

Alpha-1-acid glycoprotein

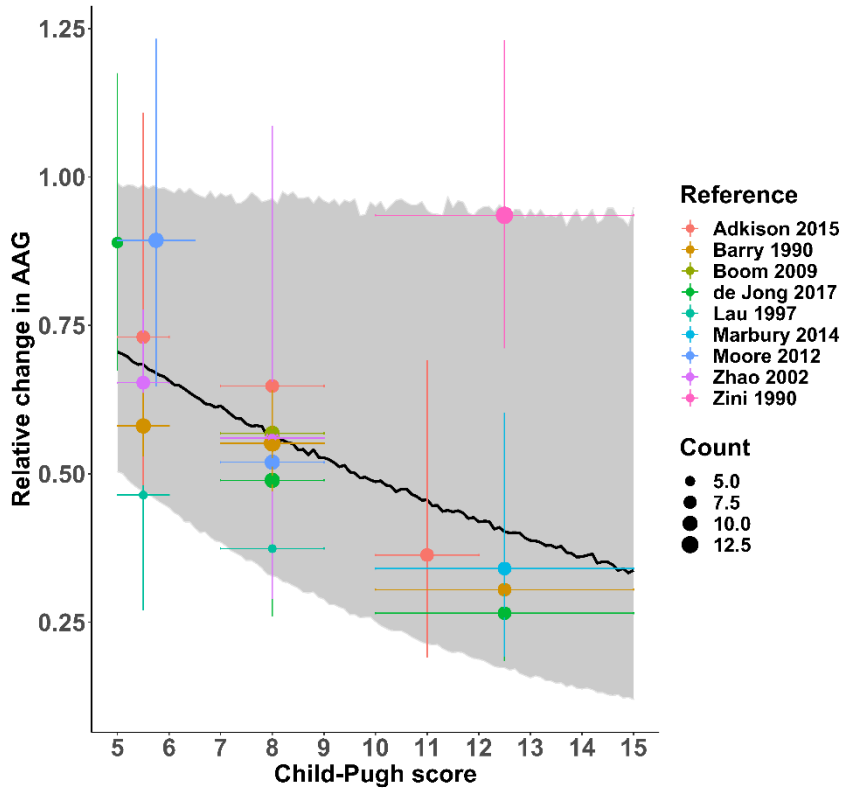

Figure source: Schneider 2024

GFR

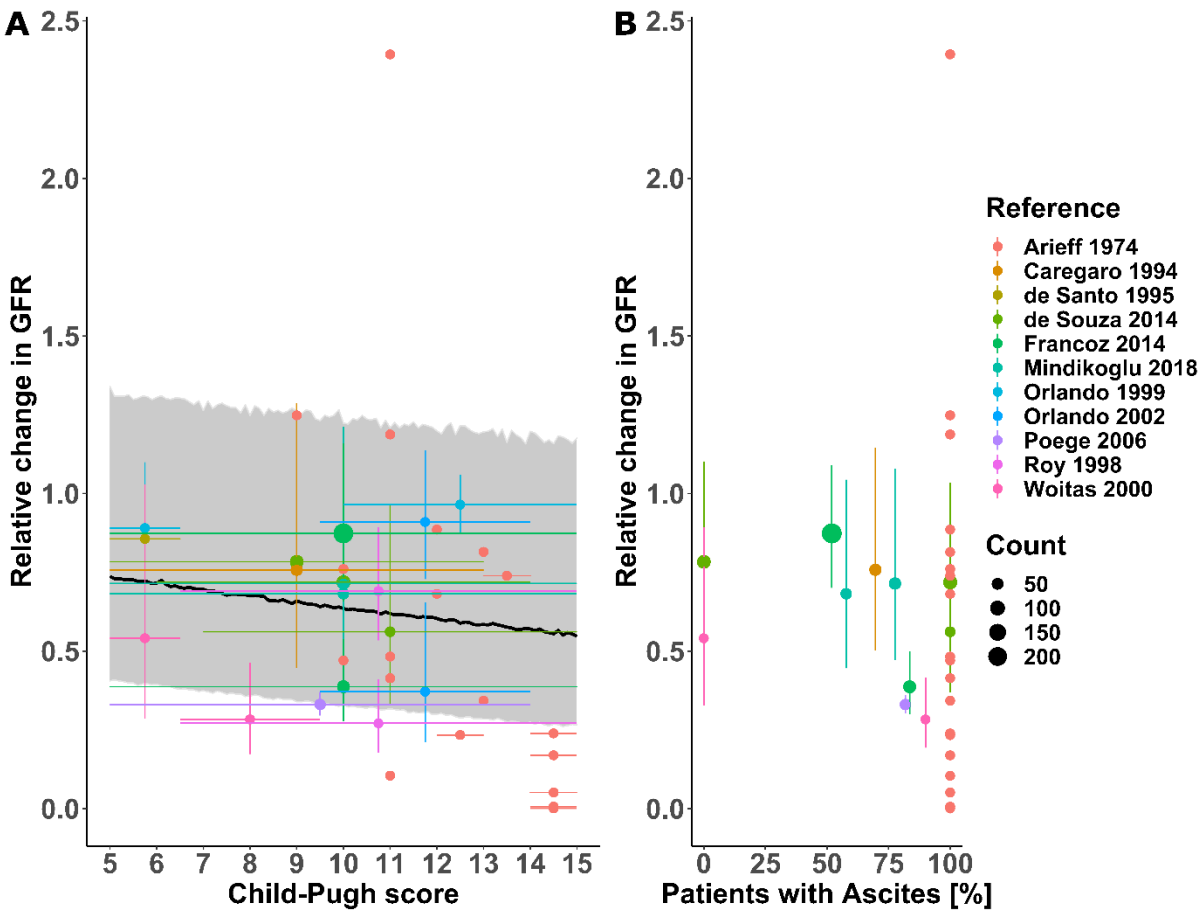

Figure source: Schneider 2024

Liver volume

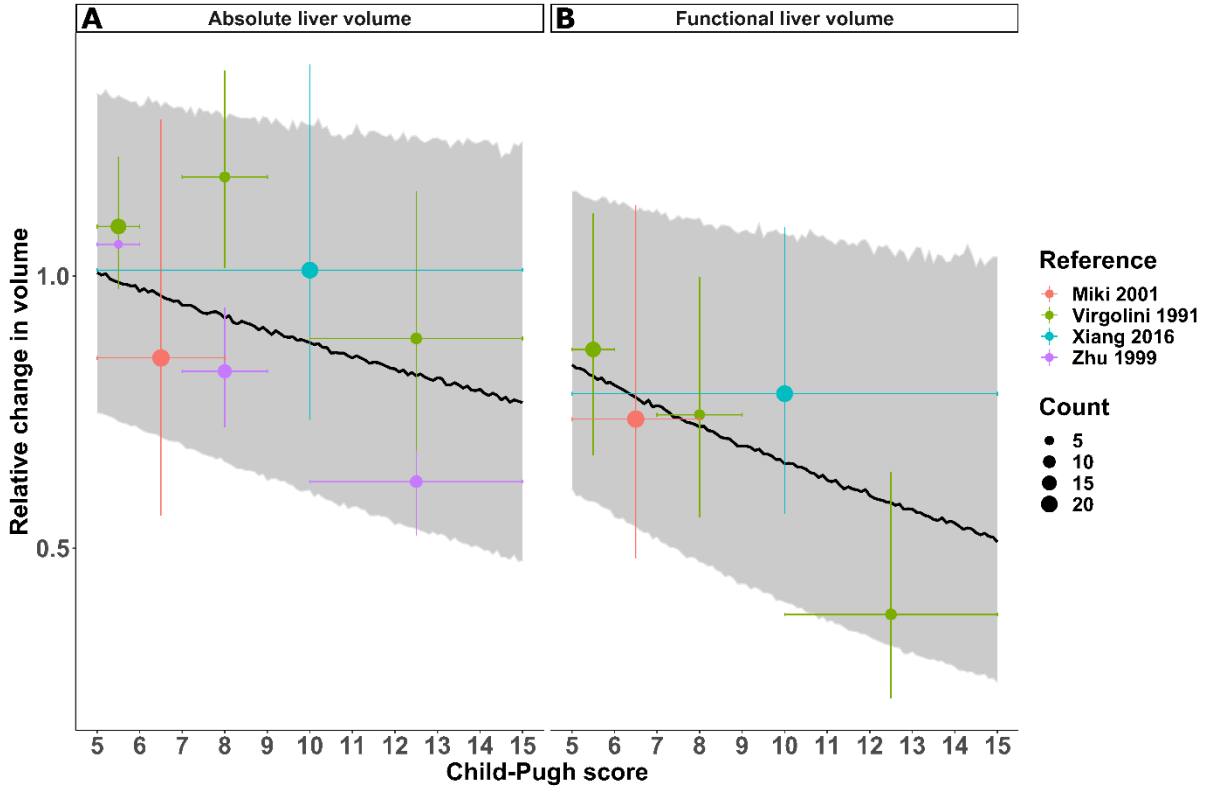

Figure source: Schneider 2024

Renal blood flow

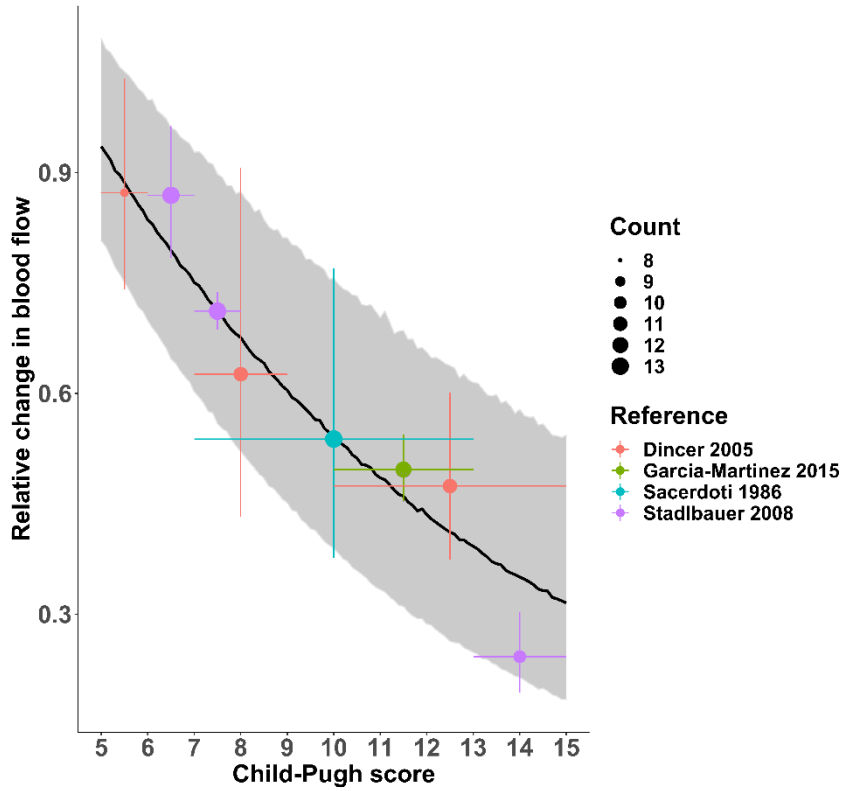

Figure source: Schneider 2024

Liver blood flow

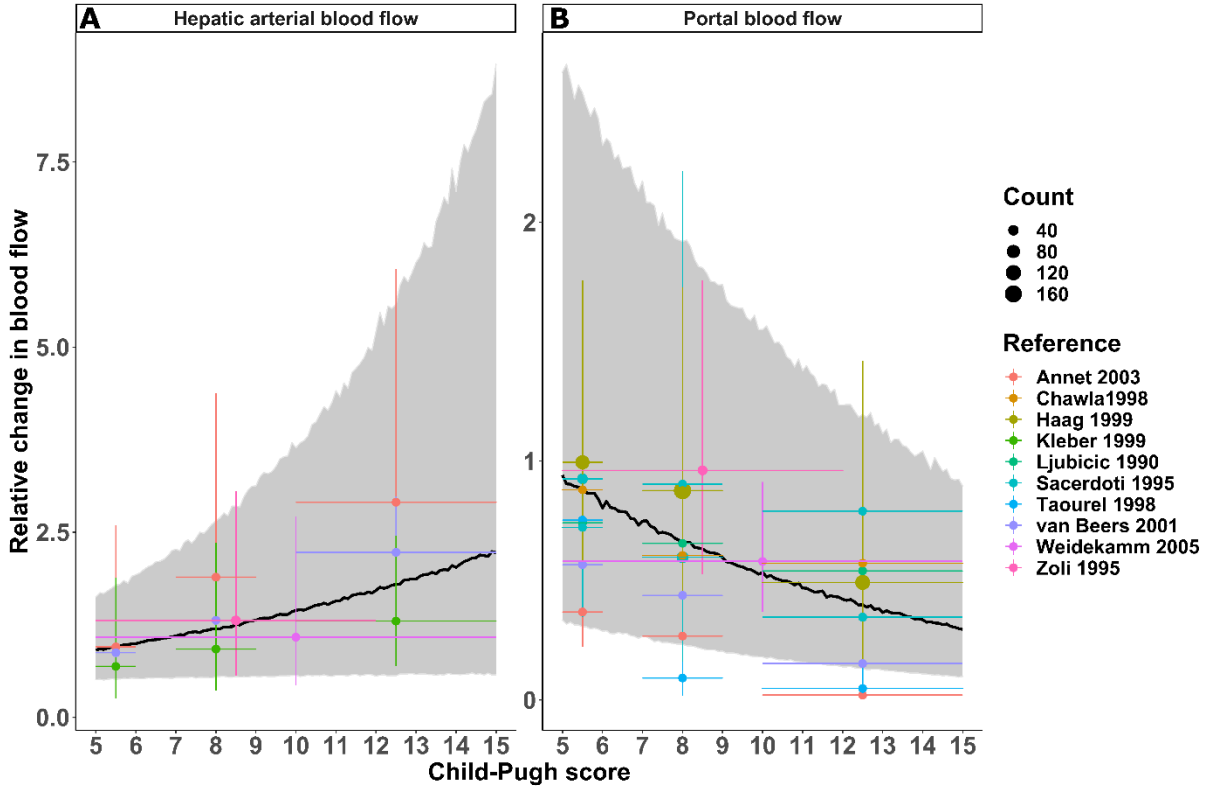

Figure source: Schneider 2024

Cardiac index

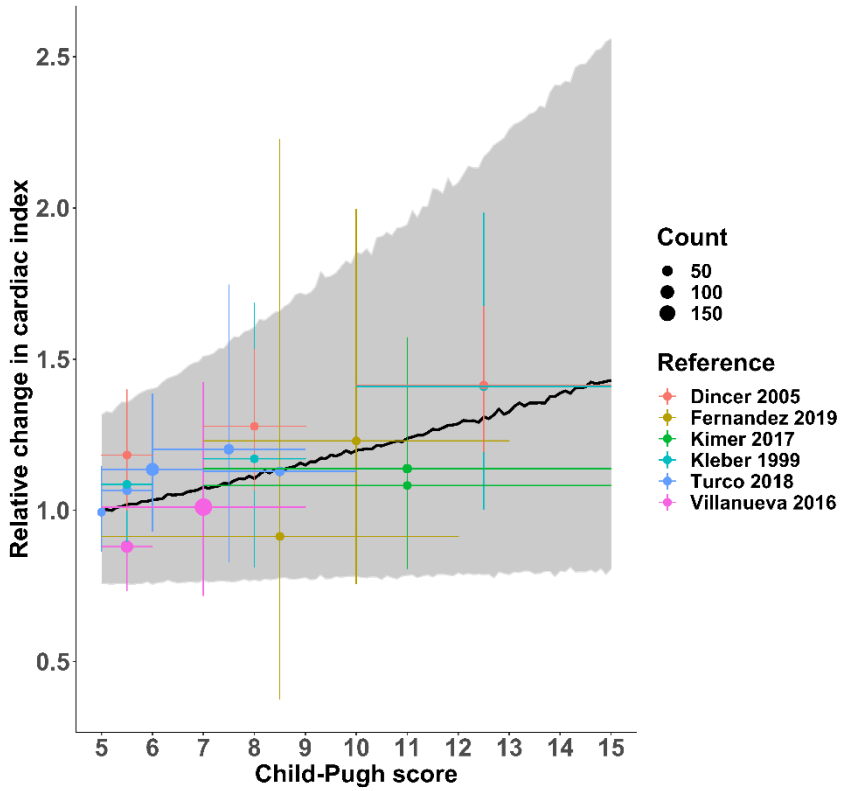

Figure source: Schneider 2024

Body compositon & ascites

Total body water

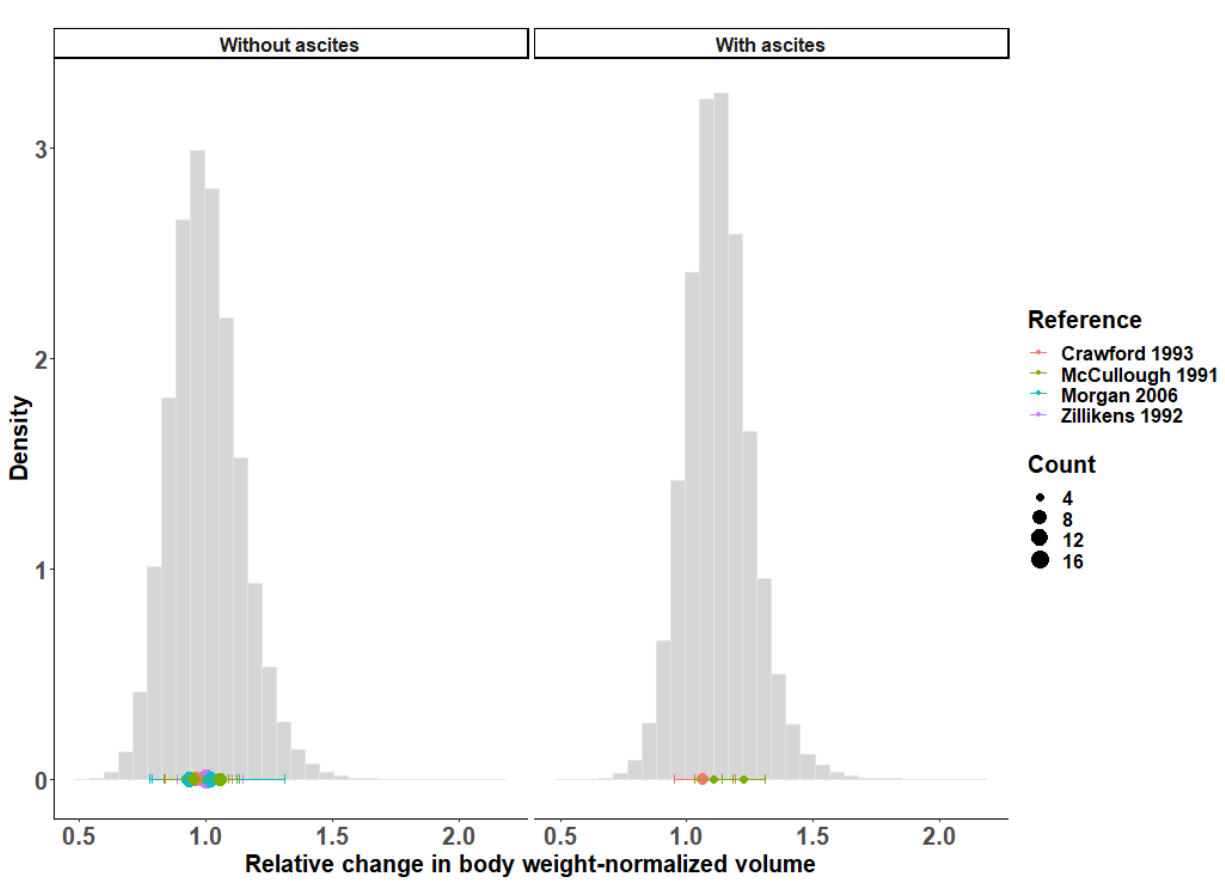

Extracellular body water

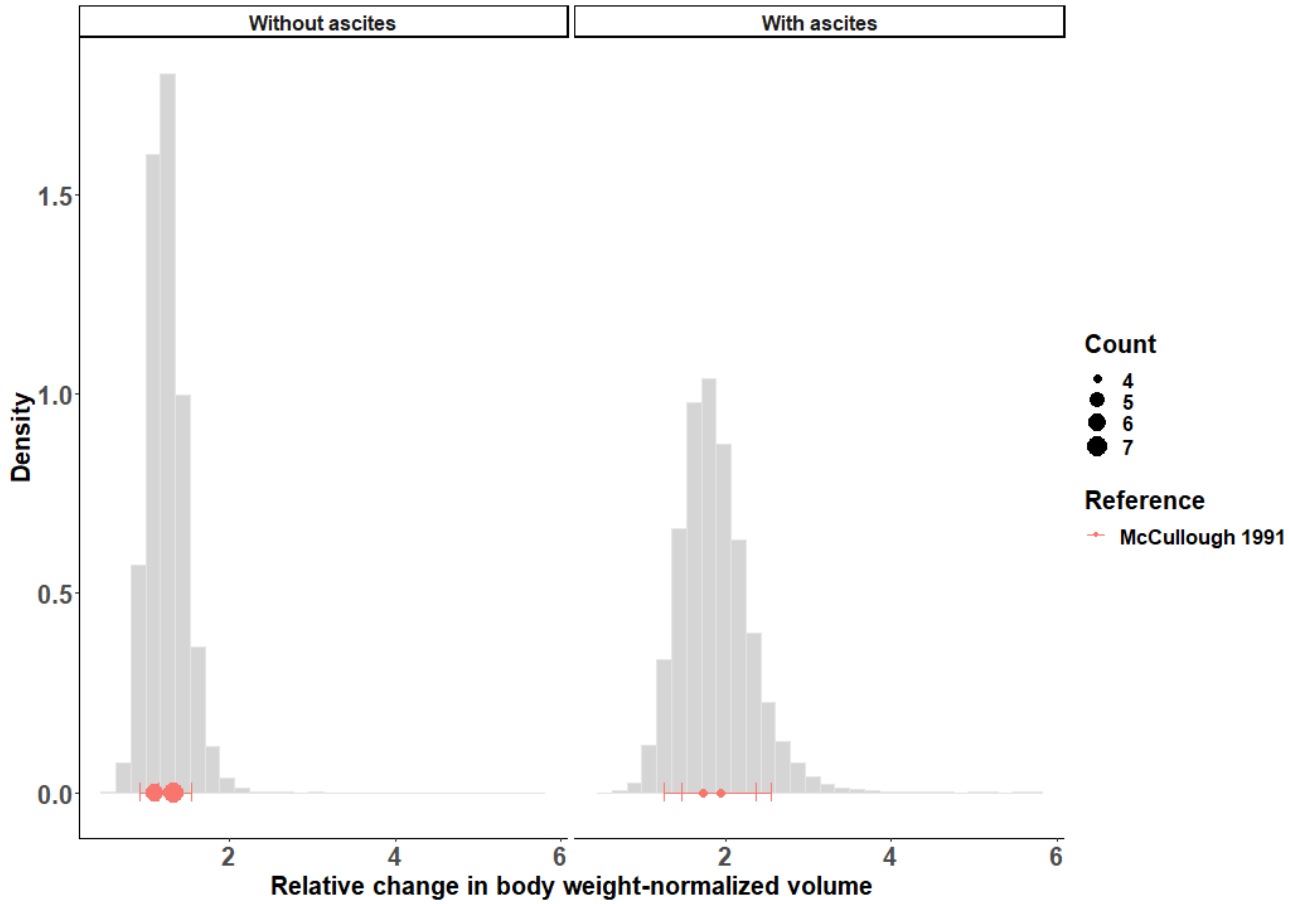

Figure source: Schneider 2024

Distribution of relevant parameters in virtual cirrhosis populations in dependency of the Child-Pugh class

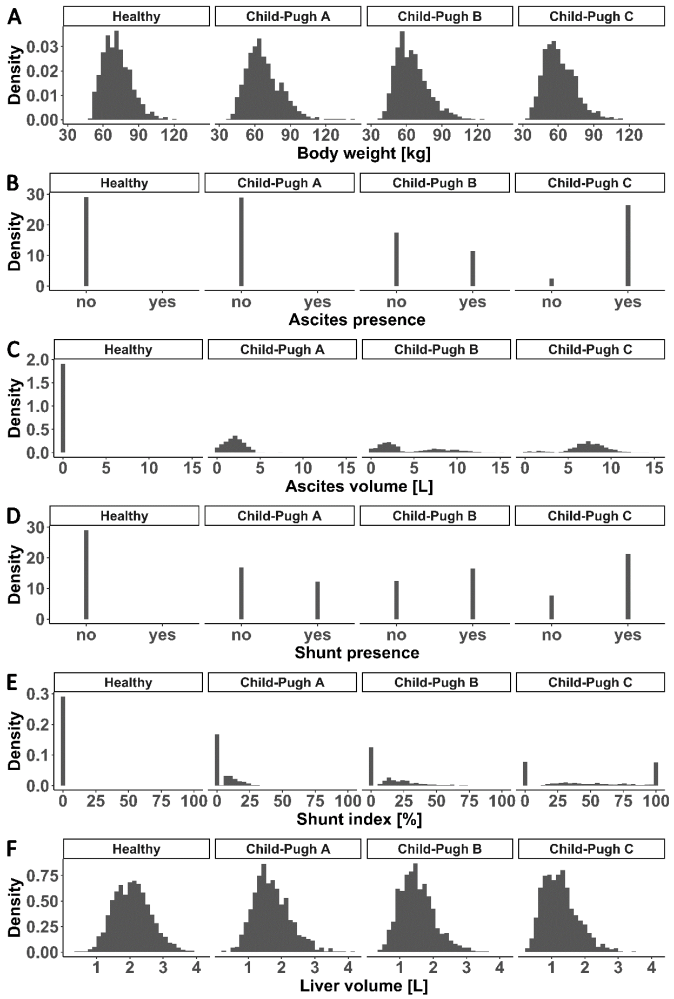

Figure source: Schneider 2024

Simulated and observed PK of tobramycin

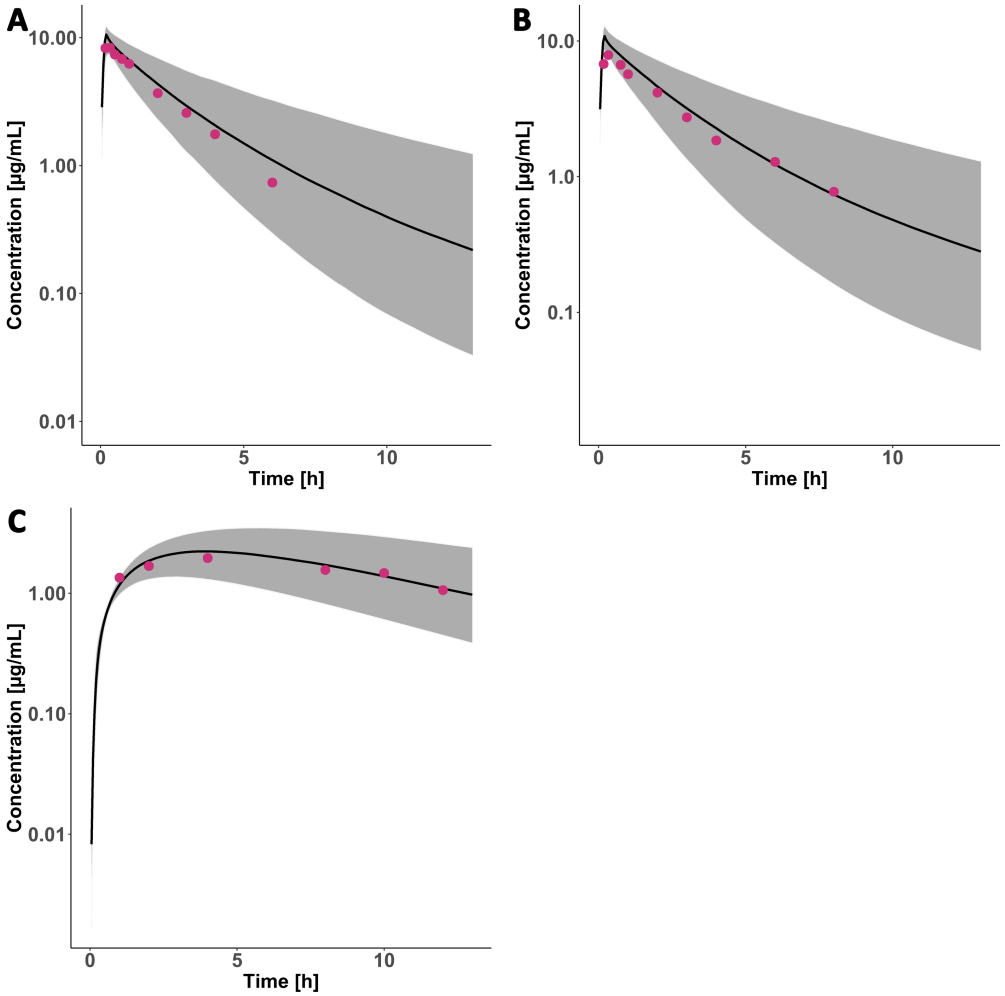

A) Plasma concentration of tobramycin in cirrhotic patient without ascites
B) Plasma concentration of tobramycin in cirrhostic patients with ascites
C) Concentration of tobramycin in the ascitic fluid

Figure source: Schneider 2024

Simulated and observed PK of tobramycin

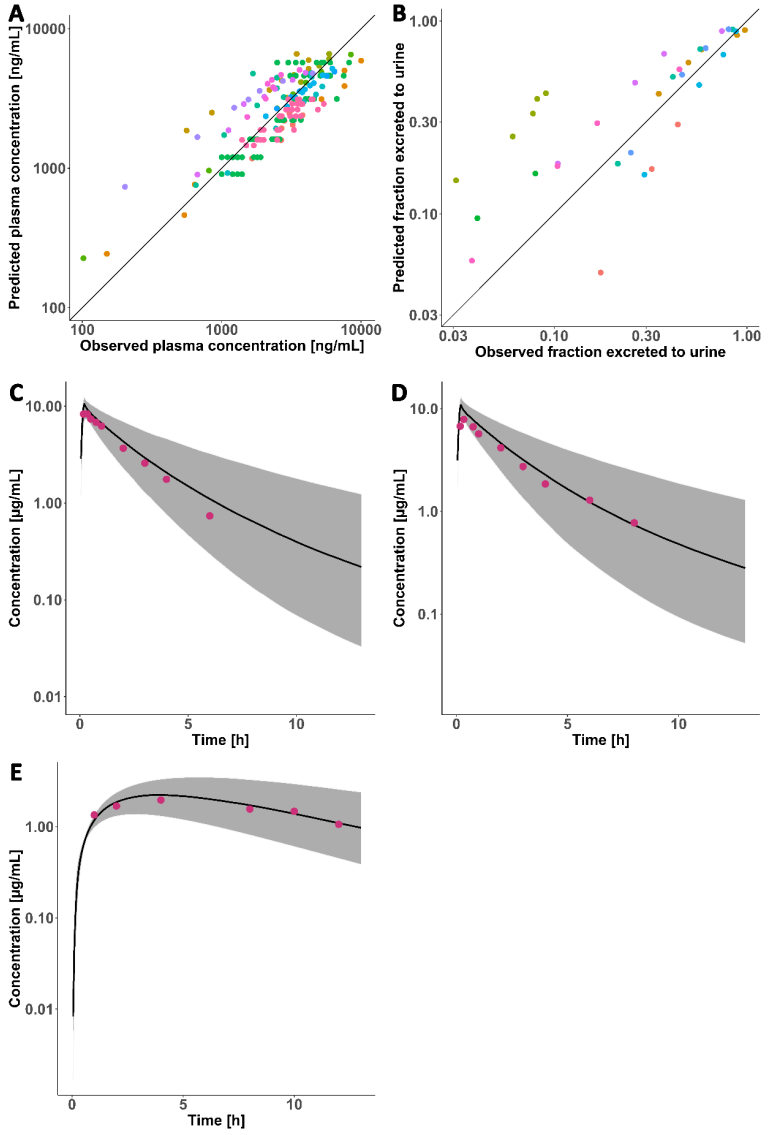

Simulated and observed PK of tobramycin

. (A, B) The model performance in non-cirrhotic subjects is depicted in predicted vs. observed plots with different colors representing different clinical studies [104-108]. The straight line represents the line of identity. The PK after IV administration of 2mg/kg of tobramycin over 10 minutes in cirrhotic patients without (C) and with (D, E) ascites are plotted as concentration-time profiles for (C, D) plasma concentrations and (E) the ascitic fluid. For the simulation with ascites, the ascites volume of all individuals of the virtual population was set to the value of 2.91L of the observed patient. Lines and bands represent median and 5th to 95th percentile, respectively. The points represent observed data from a cirrhotic patient [97]

Figure source: Schneider 2024

Midazolam

CYP3A4 substrate

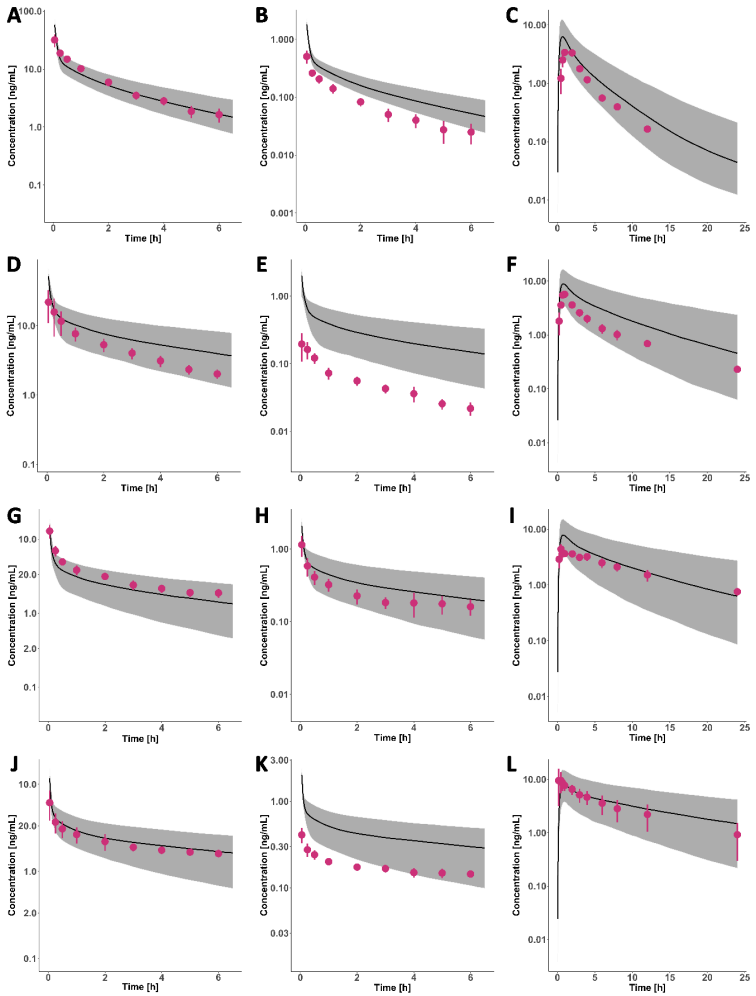

Simulated and observed PK of midazolam . The subplots depict (A, D, G, J) total and (B, E, H, K) unbound midazolam concentration after IV administration of 1mg of midazolam and (C, F, I, L) total concentration after oral administration of 2mg of midazolam in (A-C) healthy controls, (D-F) Child-Pugh A patients, (G-I) Child-Pugh B patients, and (J-L) Child-Pugh C patients. Lines and bands represent median and 5th to 95th percentile, respectively. Points and error bars represent mean ± SEM of observed data [98; 101].

Figure source: Schneider 2024

Alfentanil

CYP3A4 substrate

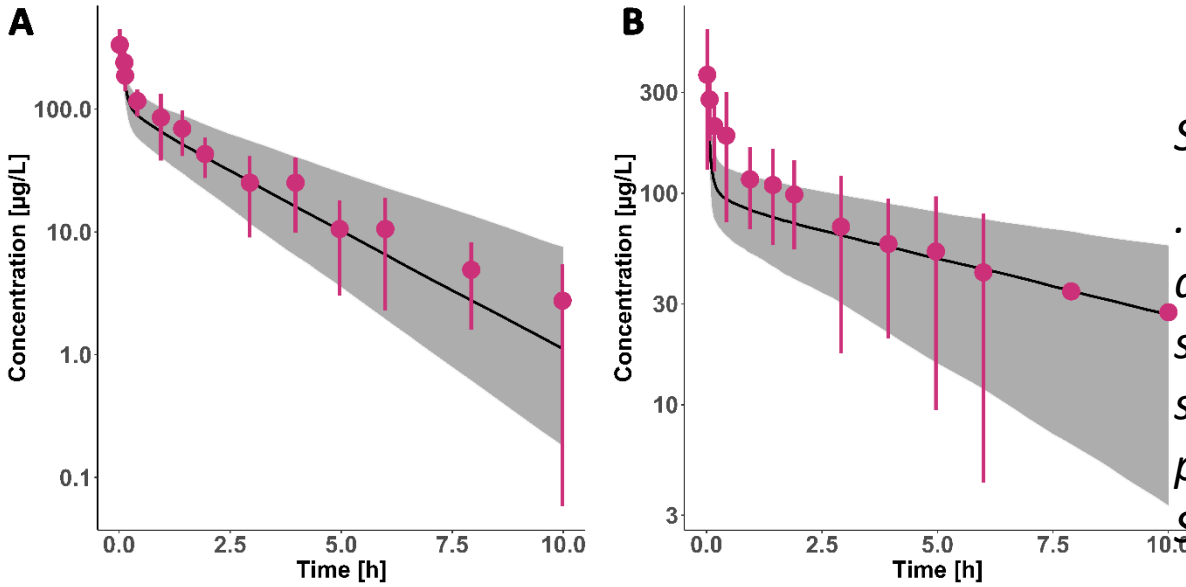

Simulated and observed PK of alfentanil

. The subplots depict alfentanil plasma concentration values after IV administration of 50µg/kg of alfentanil in (A) healthy subjects and (B) cirrhotic patients ranging from Child-Pugh score 7 to 13. Lines and bands represent median and 5th to 95th percentile, respectively. Points and error bars represent mean ± SD of observed data [99].

Figure source: Schneider 2024

Metoprolol

CYP2D6 substrate

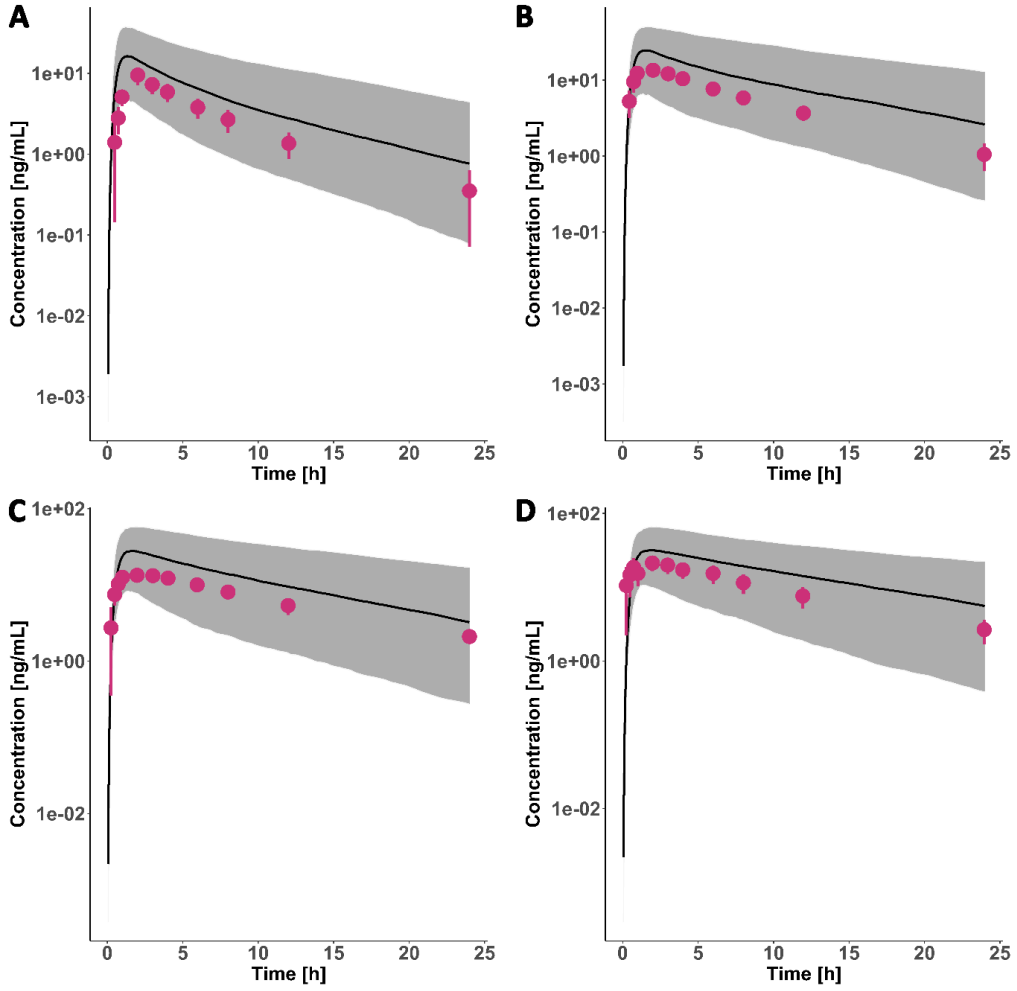

Simulated and observed PK of metoprolol . The subplots depict metoprolol plasma concentration values after oral administration of 12.5 mg of metoprolol tartrate in (A) healthy subjects, (B) Child-Pugh class A patients, (C) Child-Pugh class B patients and (D) Child-Pugh class C patients. Lines and bands represent median and 5th to 95th percentile, respectively. Points and error bars represent mean ± SEM of observed data [101].

Figure source: Schneider 2024

Omeprazole

CYP2C19 substrate

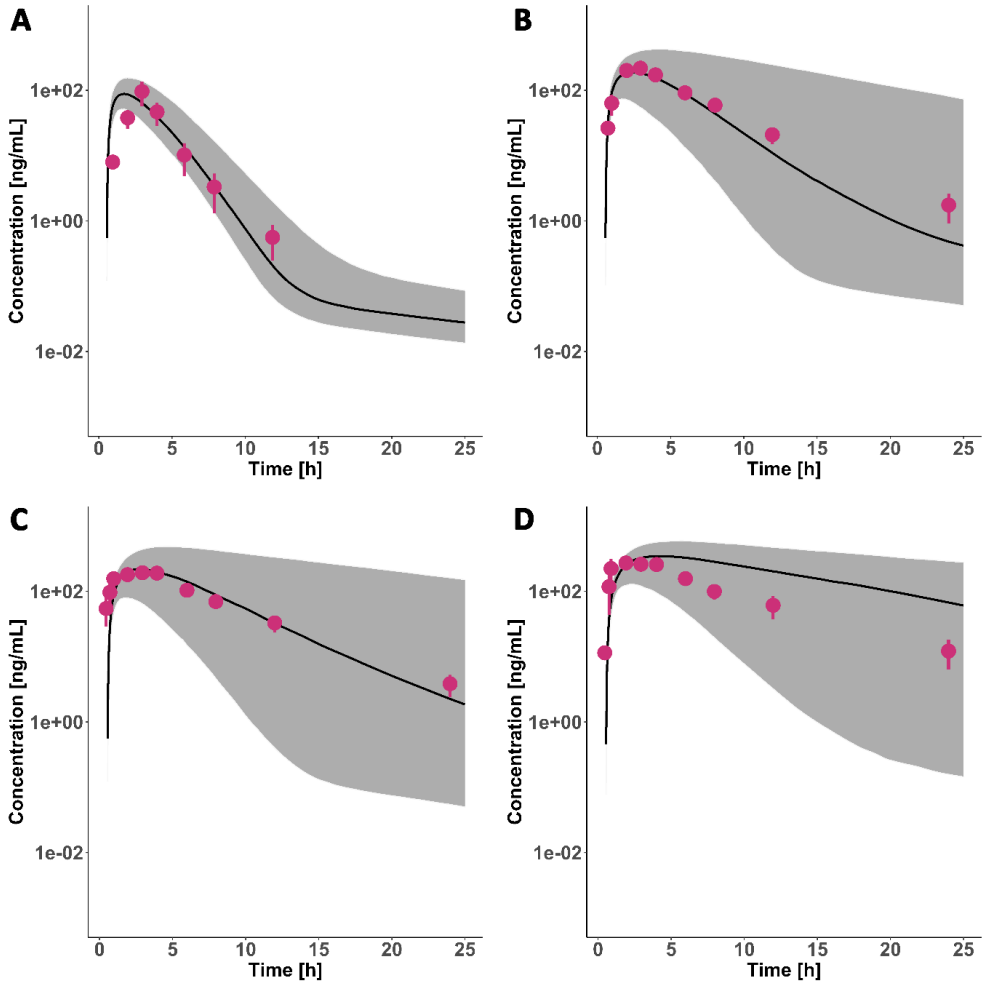

Figure source: Schneider 2024

Efavirenz

CYP2B6 substrate

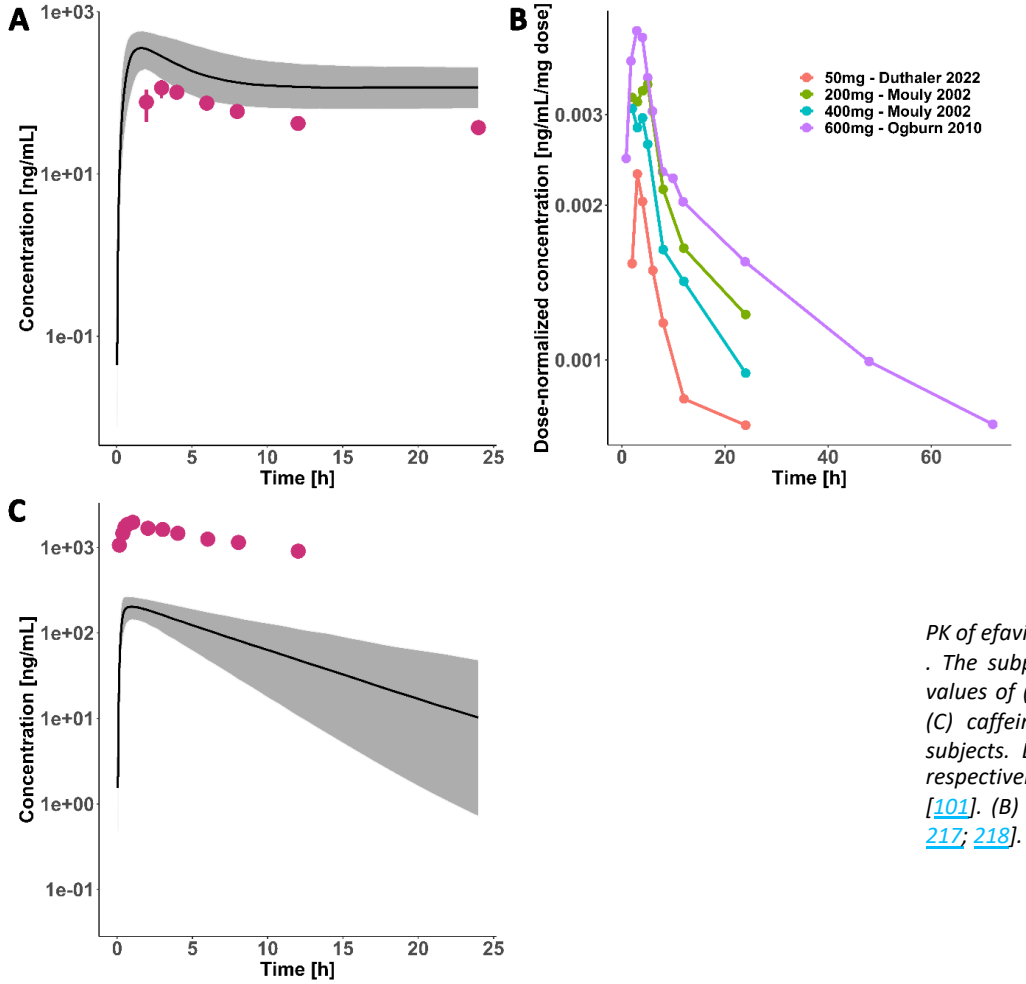

PK of efavirenz and caffeine

. The subplots depict the simulated and observed plasma concentration values of (A) efavirenz after oral administration of 50mg of efavirenz and (C) caffeine after oral administration of 10mg of caffeine in healthy subjects. Lines and bands represent median and 5th to 95th percentile, respectively. Points and error bars represent mean ± SEM of observed data [101]. (B) Dose-normalized plasma concentration data for efavirenz [101; 217; 218].

Figure source: Schneider 2024

Caffeine

CYP1A2 substrate

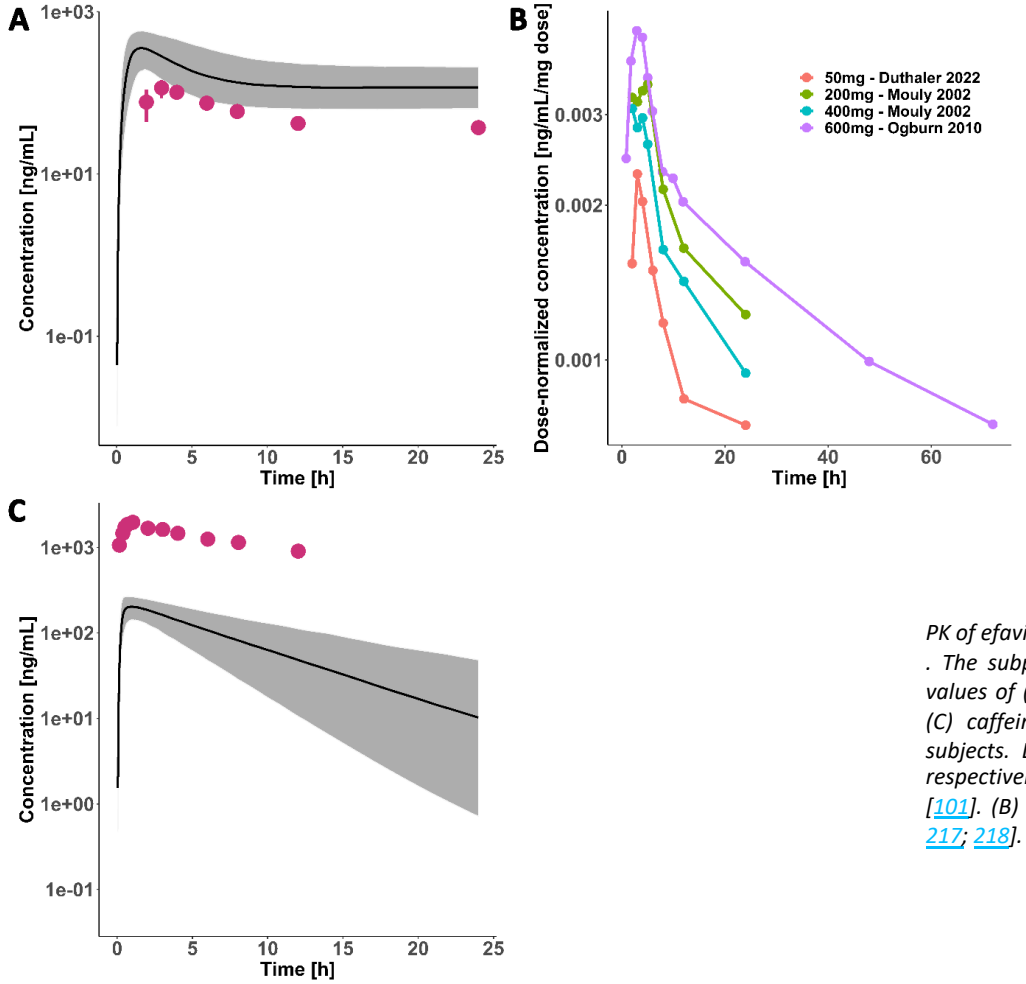

PK of efavirenz and caffeine

. The subplots depict the simulated and observed plasma concentration values of (A) efavirenz after oral administration of 50mg of efavirenz and (C) caffeine after oral administration of 10mg of caffeine in healthy subjects. Lines and bands represent median and 5th to 95th percentile, respectively. Points and error bars represent mean ± SEM of observed data [101]. (B) Dose-normalized plasma concentration data for efavirenz [101; 217; 218].

Figure source: Schneider 2024